Injectable non-immunogenic PEG-like conjugate that forms a subcutaneous depot and enables sustained delivery of a peptide drug

Imran Ozer[1], Anna Slezak[2†], Jeffrey I. Everitt[3], Xinghai Li[1], Nikita Zakharov[1], Joel H. Collier[1], Jonathan E. Campbell[4,5,6], David A. D'Alessio[4,5], and Ashutosh Chilkoti[1*]

[1]Department of Biomedical Engineering, Duke University, Durham, North Carolina 27708, USA.

[2]Department of Chemistry, Duke University, Durham, North Carolina 27708, USA.

[3]Department of Pathology, Duke University Medical Center, Durham, North Carolina 27701, USA.

[4]Duke Molecular Physiology Institute, Duke University, Durham, North Carolina 27701, USA

[5]Division of Endocrinology, Duke University Medical Center, Durham, North Carolina, 27701, USA.

[6]Department of Pharmacology and Cancer Biology, Duke University, Durham, NC, USA.

[†]Present Address: Pritzker School of Molecular Engineering, University of Chicago, Chicago, Illinois, 60637, USA.

*e-mail: chilkoti@duke.edu

Table of Contents

Section 1. Synthesis and characterization of POEGMA library.

Synthesis, purification, and characterization of an azide-functional amide-based polymerization initiator.

2-Bromoisobutanoic acid N-hydroxy succinimide ester (4.1 mmol; 1.14 g) was purged with argon and dissolved in 5 ml anhydrous dichloromethane (DCM) (Flask 1). In a separate Schlenk flask (Flask 2), 3-azido-1-propanamine (4.9 mmol; 0.52 g) was purged with argon and dissolved in 11.09 ml anhydrous DCM, followed by cooling to 0^{o}C in an ice bath. The solution in Flask 1 was then added dropwise to Flask 2 under an inert atmosphere. The resulting solution was kept on ice for 30 min and left stirring at 30^{o}C for 12 h. The solution was diluted in DCM and passed through a polyvinylidene fluoride (PVDF) membrane to remove the solid phase. The resulting clear solution was washed with 0.5N HCl, saturated Na_2HCO_3, and 1M NaCl, respectively, and the organic phase was collected. The organic phase dried over anhydrous $MgSO_4$, followed by filtration through a PVDF membrane and DCM evaporation under vacuum, yielding the polymerization initiator. The polymerization initiator was characterized by high-resolution mass spectrometry (HRMS) using an Agilent G6224 liquid chromatography mass spectrometry-time of flight (LCMS-TOF) using an electrospray ionization source (Agilent) and a Series 1200 high-pressure liquid chromatography (HPLC) (Agilent) **(Supplementary Fig. 1)** and nuclear magnetic resonance (NMR) spectroscopy using a 400 MHz Varian Inova spectrometer and an ACD/NMR analysis software (ACD Labs) **(Supplementary Fig. 2)**.

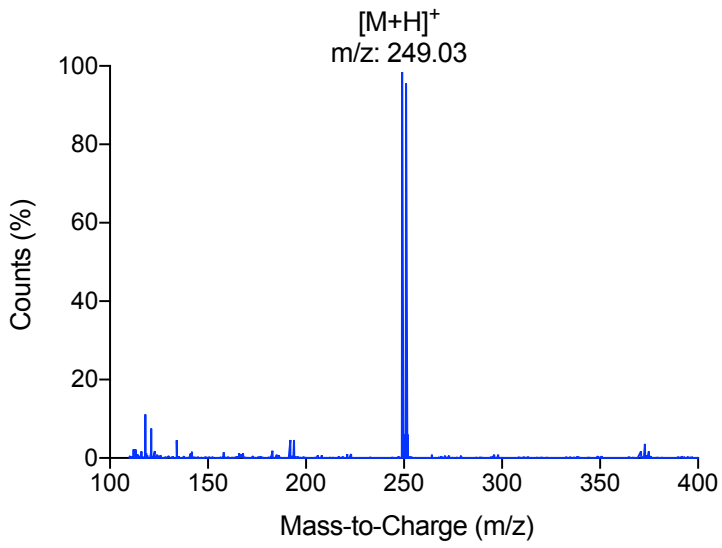

Supplementary Figure 1. HRMS of the azide-functional amide-based polymerization initiator. The initiator was analyzed using reverse-phase HPLC on an Agilent G6224 LCMS-TOF using a Series 1200 HPLC (Agilent) equipped with a diode array detector (Agilent) operating at 254 nm and connected to an electrospray ionization source (Agilent) operating in positive ion mode. 5 µl of the polymerization initiator was diluted 1:20,000 (v/v) in methanol and separated on a Phenomenex Kinetix C18 column (3 mm internal diameter x 30 mm length, 2.6 µm particle size) at 40°C. Mobile phase A and B consisted of 100:3:0.4 (v/v) water: methanol: formic acid and 100:3:0.3 (v/v) acetonitrile: water: formic acid, respectively. Mobile phase B was 0% for 2 min, with a linear gradient to 95% for 10 min, and held at 95% for 3 min. The flow rate was 0.35 ml min^{-1}. The major peak at 249.03 Da was assigned as the $[M+H]^+$ ion, based on the initiator's theoretical mass (M) of 248.03 Da.

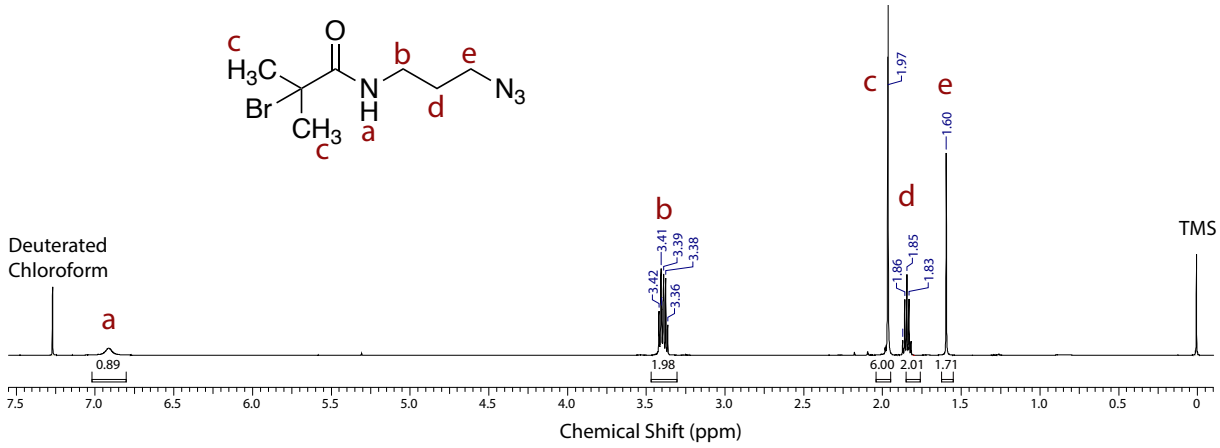

Supplementary Figure 2. NMR spectrum of the azide functional amide-based polymerization initiator. Data were acquired using a 400 MHz Varian Inova spectrometer and analyzed using ACD/NMR software (ACD Labs). Deuterated chloroform and tetramethylsilane (TMS) were used as a solvent and reference, respectively.

Characterization of EG2 and EG3 monomers

Triethylene glycol methyl ether methacrylate (EG3) and diethylene glycol methyl ether methacrylate (EG2) monomers characterized using HRMS using an Agilent G6224 LCMS-TOF using an electrospray ionization source (Agilent) and a Series 1200 HPLC (Agilent) **(Supplementary Figures 3 and 5)** and NMR spectrometry using a 400 MHz Varian Inova spectrometer and an ACD/NMR analysis software (ACD Labs) **(Supplementary Figures 4 and 6)**.

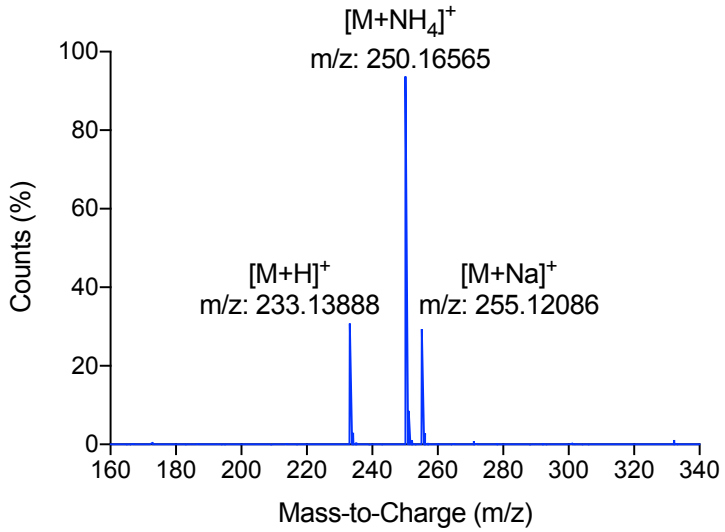

Supplementary Figure 3. HRMS of EG3 monomer. EG3 monomer was characterized using reverse-phase HPLC on an Agilent G6224 LCMS-TOF using a Series 1200 HPLC (Agilent) equipped with a diode array detector (Agilent) operating at 254 nm and connected to an electrospray ionization source (Agilent) operating in positive ion mode. 5 µl of the monomer was diluted 1:20,000 (v/v) in water/acetonitrile and separated on a Phenomenex Kinetix C18 column (3 mm ID x 30 mm length, 2.6 µm particle size) at 40°C. Mobile phase A and B consisted of 100:3:0.4 (v/v) water: methanol: formic acid and 100:3:0.3 (v/v) acetonitrile: water: formic acid, respectively. Mobile phase B was 0% for 2 min, with a linear gradient up to 95% from 8 min, and was then held at 95% for 5 min. The flow rate was 0.35 ml min^{-1}. Based on the EG3 monomer's theoretical mass (M) of 212.13 Da, the major peaks at 233.13, 250.16, and 255.12 Da were assigned as the $[M+H]^+$, $[M+NH_4]^+$, and $[M+Na]^+$ ions, respectively.

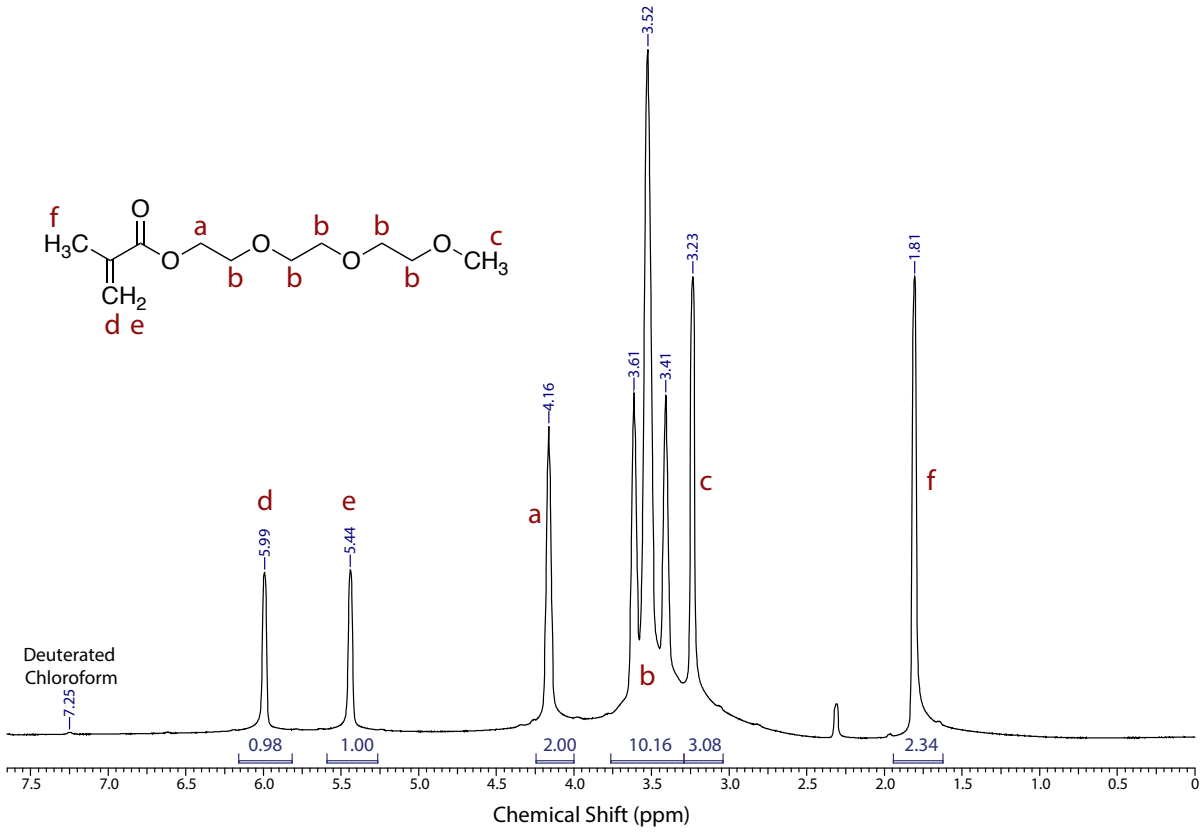

Supplementary Figure 4. NMR spectrum of EG3 monomer. Data were acquired on a 400 MHz Varian Inova NMR spectrometer and analyzed using ACD/NMR software (ACD Labs). Deuterated chloroform was used as the solvent.

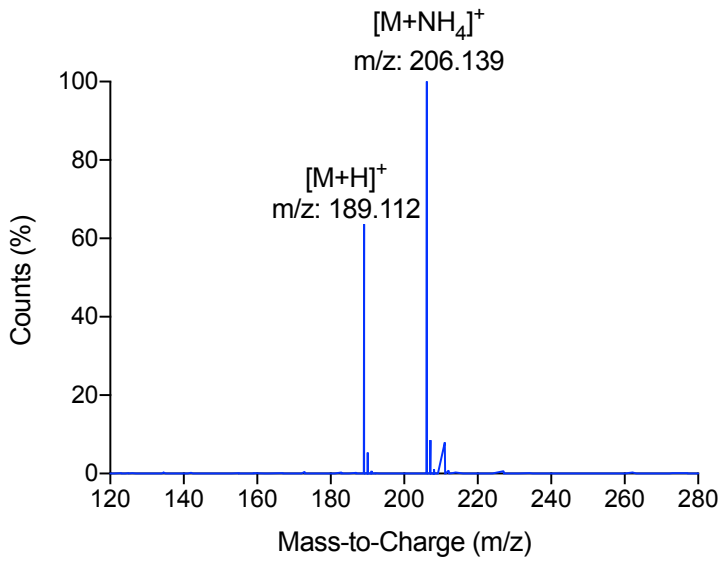

Supplementary Figure 5. HRMS of EG2 monomer. The monomer was characterized using reverse-phase HPLC on an Agilent G6224 LCMS-TOF using a Series 1200 HPLC (Agilent) equipped with a diode array detector (Agilent) operating at 254 nm and connected to an electrospray ionization source (Agilent) operating in positive ion mode. 5 µl of the monomer was diluted 1:20,000 (v/v) in water/MeCN and separated on a Phenomenex Kinetix C18 column (3 mm ID x 30 mm length, 2.6 µm particle size) at 40°C. The mobile phases A and B consisted of 100:3:0.4 (v/v) water: MeOH: formic acid and 100:3:0.3 (v/v) MeCN: water: formic acid, respectively. Mobile phase B was 0% from 0-2 min, then gradually ramped up to 95% from 2-10 min, held at 95% for 10-15 min. The flow rate was 0.35 ml min^{-1}. The major peaks at 189.1 and 209.1 were assigned as $[M+H]^+$ and $[M+NH_4]^+$ ions based on the EG2 monomer's theoretical mass (M) of 188.1 Da.

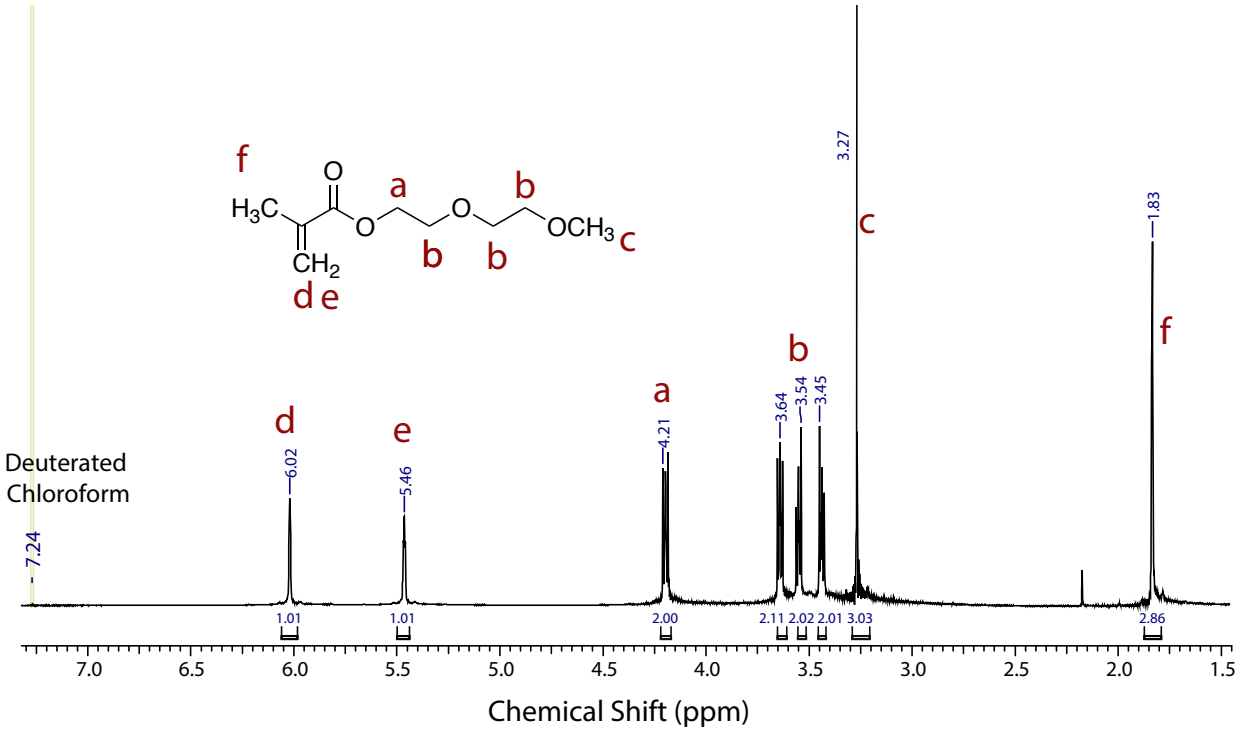

82

83 **Supplementary Figure 6. NMR spectrum of EG2 monomer.** Data were acquired using a 400 MHz Varian Inova NMR spectrometer

84 and analyzed using ACD/NMR software (ACD Labs). Deuterated chloroform was used as the solvent.

Supplementary Table 1. Summary of POEGMA library characterization. The monomer composition of the POEGMAs was defined as the mole percentage of EG2 (or EG3) content in the copolymer derived from the NMR spectra shown in Supplementary Fig. 7-8. The DP, M_n, M_w, and $Đ$ were determined from GPC-MALS data shown in Supplementary Fig. 9. The R_h was calculated from DLS data shown in Supplementary Fig. 10. T_t was derived from UV-vis spectrophotometry curves shown in Fig. 1b-d.

Group	POEGMA ID	EG2% by NMR	DP	M_w	M_n	$Đ(M_w/M_n)$	R_h(nm)	Tt (25μM;°C)
$EG3_{100\%}$	P1	0	105	24.7	22.7	1.079	3.4 ± 0.6	51.6
	P2	0	194	45.3	40.3	1.123	4.6 ± 1.0	48.9
	P3	0	314	73.2	68.0	1.075	6.5 ± 1.4	46.7
	P4	0	386	90.0	84.7	1.063	6.7 ± 1.3	43.9
$EG2_{58\%}$	P5	58.4	95	19.9	18.3	1.088	3.0 ± 0.5	37.8
	P6	58.5	206	42.7	39.6	1.078	3.4 ± 0.4	35.8
	P7	59.0	285	59.1	53.1	1.113	4.8 ± 1.2	33.8
	P8	56.5	394	82.0	71.6	1.146	5.1 ± 0.4	31.7
$EG2_{66\%}$	P9	65.6	96	19.8	18.1	1.092	2.9 ± 0.3	35.2
	P10	65.0	201	41.2	38.6	1.066	3.2 ± 0.4	33.6
	P11	68.8	298	60.5	55.3	1.095	3.9 ± 0.3	31.8
	P12	65.0	389	79.5	69.4	1.145	5.3 ± 0.7	30.6
$EG2_{74\%}$	P13	72.0	104	21.1	19.3	1.091	3.1 ± 0.4	33.7
	P14	75.5	208	41.6	38.3	1.086	3.5 ± 0.3	32.0
	P15	76.5	313	62.5	55.7	1.122	4.6 ± 0.8	30.3
	P16	73.8	420	84.2	72.2	1.166	5.7 ± 1.1	28.7
$EG2_{82\%}$	P17	82.3	105	20.8	19.0	1.097	3.1 ± 0.7	32.6
	P18	82.0	195	38.4	34.9	1.099	3.8 ± 0.5	30.1
	P19	83.0	289	56.8	52.8	1.075	4.3 ± 0.5	28.8
	P20	82.3	404	79.4	67.7	1.173	5.9 ± 1.3	26.7
$EG2_{90\%}$	P21	89.6	103	20.1	18.2	1.102	3.0 ± 0.5	30.8
	P22	92.0	210	40.6	35.3	1.151	3.5 ± 0.3	28.9
	P23	90.0	315	61.0	55.2	1.105	4.1 ± 0.5	27.0
	P24	90.0	405	78.2	66.2	1.182	4.8 ± 0.4	25.0
$EG2_{100\%}$	P25	100	190	36.0	32.3	1.116	3.1 ± 0.5	25.8

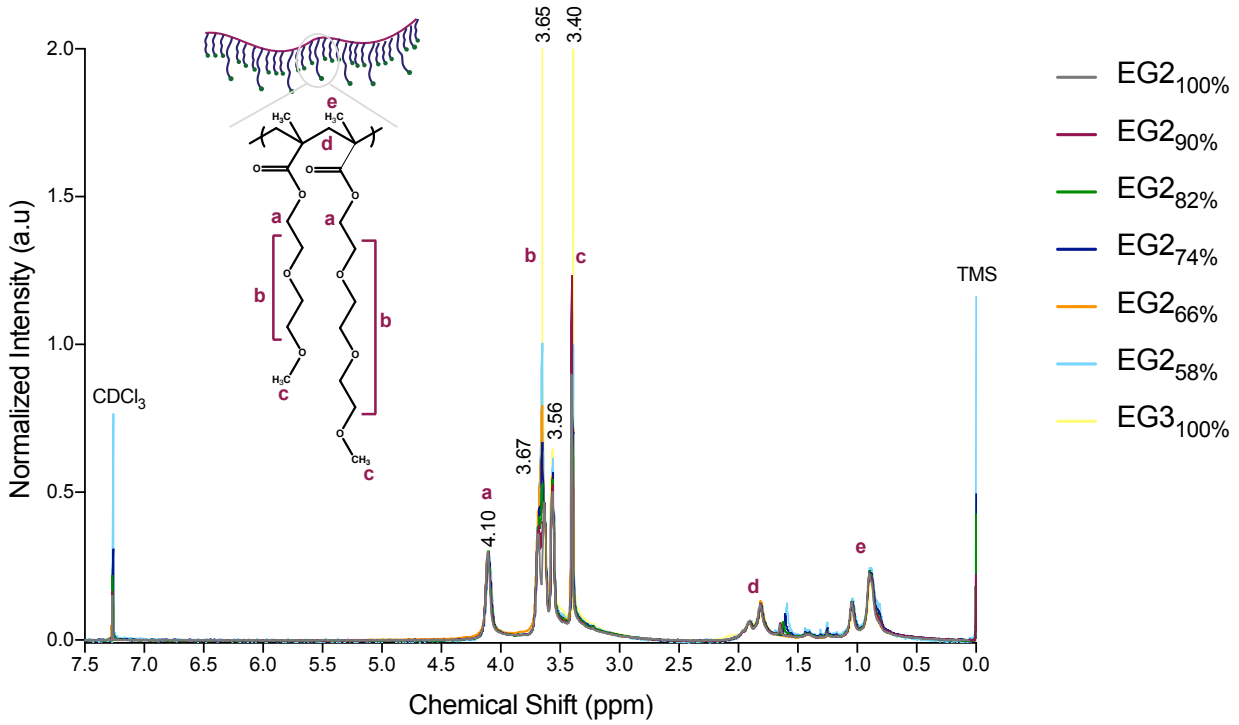

Supplementary Figure 7. Structure of POEGMAs. The POEGMA structure was identified by NMR spectroscopy at indicated monomer compositions for a DP of ~ 200. These polymers correspond to POEGMA IDs of P2, P6, P10, P14, P18, P22, and P25, shown in Supplementary Table 1. Data were acquired using a 400 MHz Varian Inova NMR spectrometer and analyzed using ACD/NMR software (ACD Labs). Deuterated chloroform ($CDCl_3$) and TMS were used as the solvent and reference.

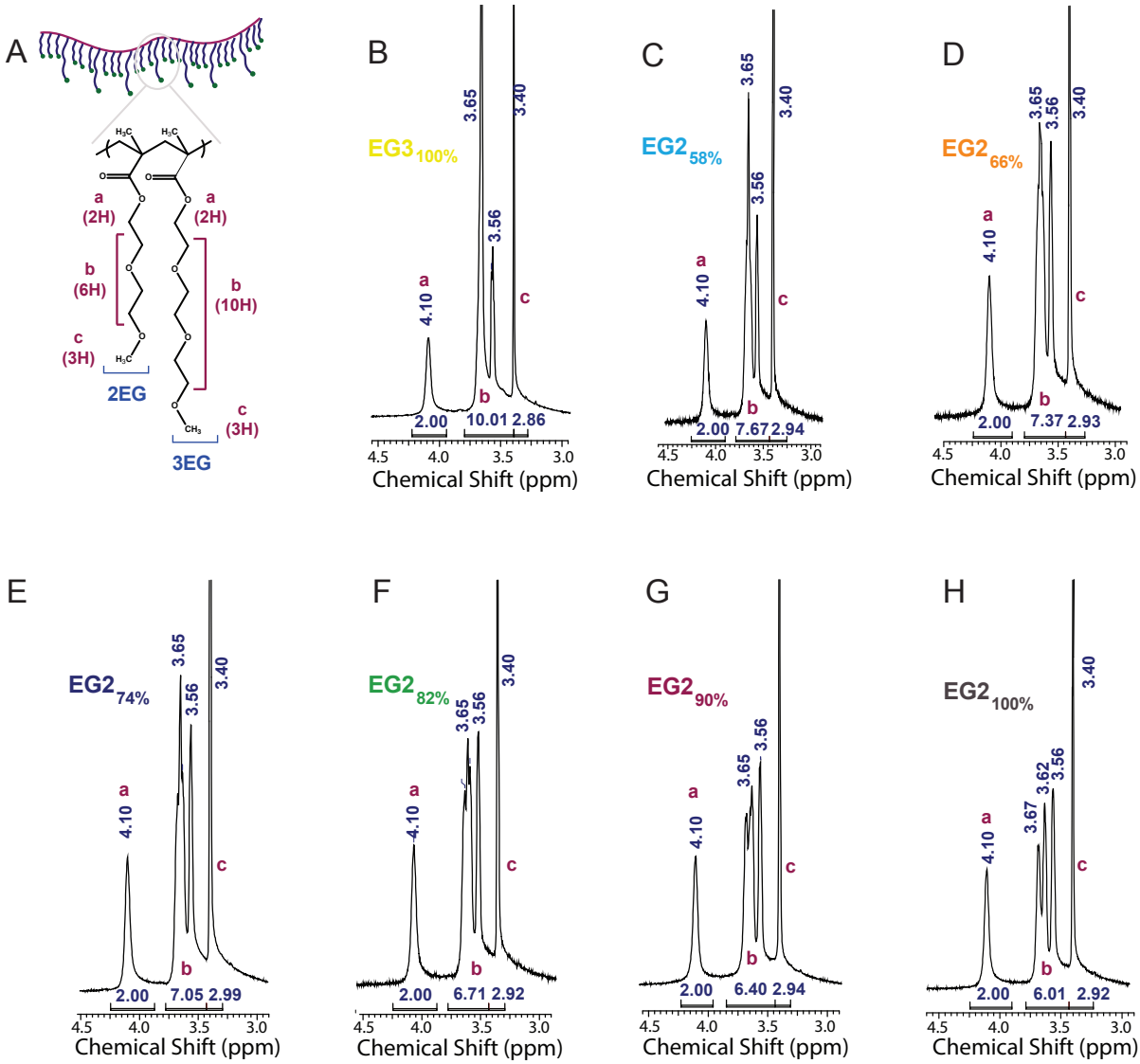

Supplementary Figure 8. The monomer composition of the POEGMA library. (A) Structure of a POEGMA copolymer. The monomer composition of **(B)** $EG3_{100\%}$, **(C)** $EG2_{58\%}$, **(D)** $EG2_{66\%}$, **(E)** $EG2_{74\%}$, **(F)** $EG2_{82\%}$, **(G)** $EG2_{90\%}$ and **(H)** $EG2_{100\%}$). These polymers correspond to POEGMA IDs of P2, P5, P9, P16, P17, P23, and P25 given in Supplementary Table 1, respectively. The monomer composition was defined as the percentage of EG2 (or EG3) content in the copolymer and characterized using NMR spectroscopy. The monomer composition was calculated from the integral value that corresponds to the average number of hydrogens (H) present in the OEG side-chain (b; 3.4-4.4 ppm; 6H for $EG2_{100\%}$ homopolymer; 10H for $EG3_{100\%}$ homopolymer) except chain end-group (c; 3.5-3.3 ppm; 3H) and methylene protons (a; 4.0-4.4 ppm; 2H).

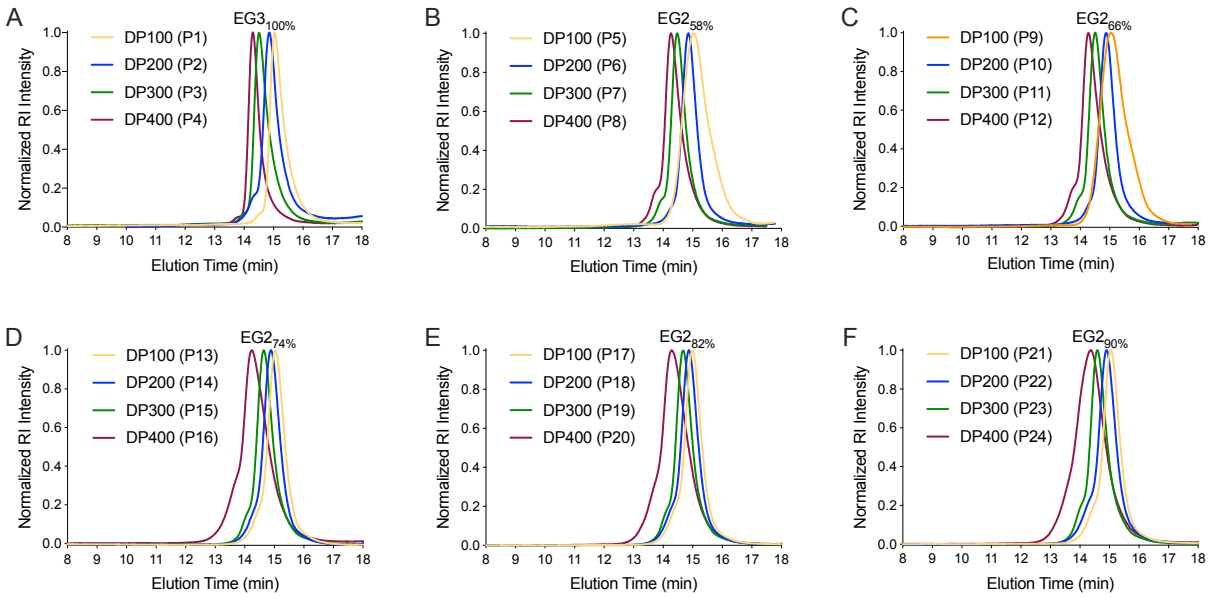

103

104 **Supplementary Figure 9. GPC traces of POEGMA library.** POEGMAs at indicated DP and compositions were separated on a GPC

105 column. The refractive index (RI) signal at 658 nm was plotted as a function of the HLPLC elution time.

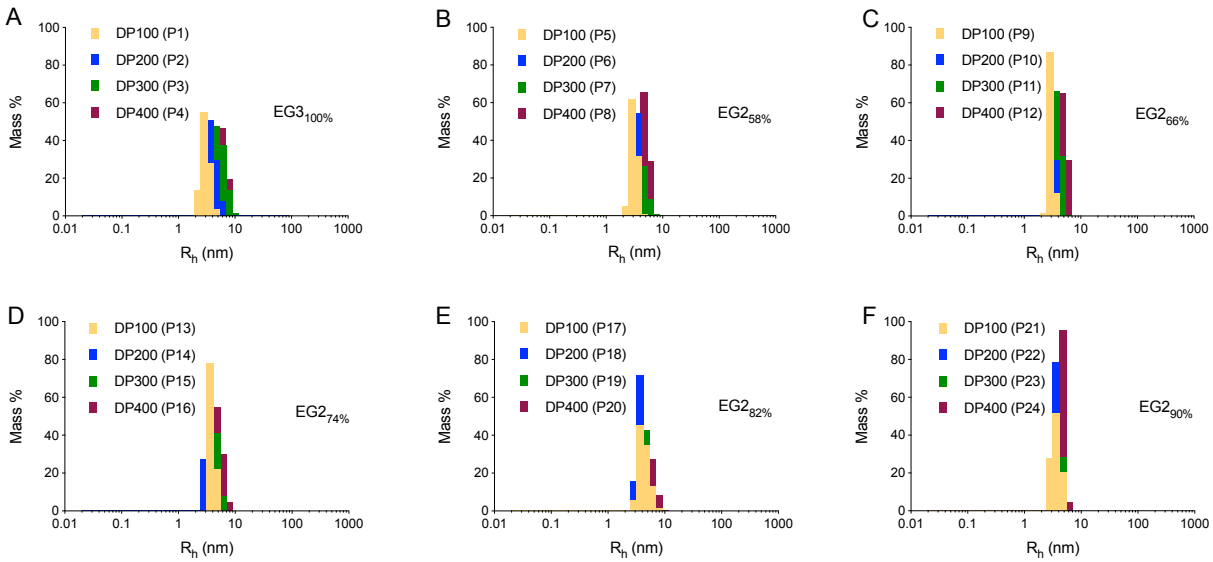

106

107 **Supplementary Figure 10. The R_h of the POEGMA library.** The R_h of **(A)** $EG3_{100\%}$, **(B)** $EG2_{58\%}$, **(C)** $EG2_{66\%}$, **(D)** $EG2_{74\%}$, **(E)** $EG2_{82\%}$,

108 and **(F)** $EG2_{90\%}$ were characterized at varying DP by DLS on a temperature-controlled DynaPro Plate Reader (Wyatt Technologies).

Section 2. Synthesis and characterization of site-specific and stoichiometric exendin conjugates.

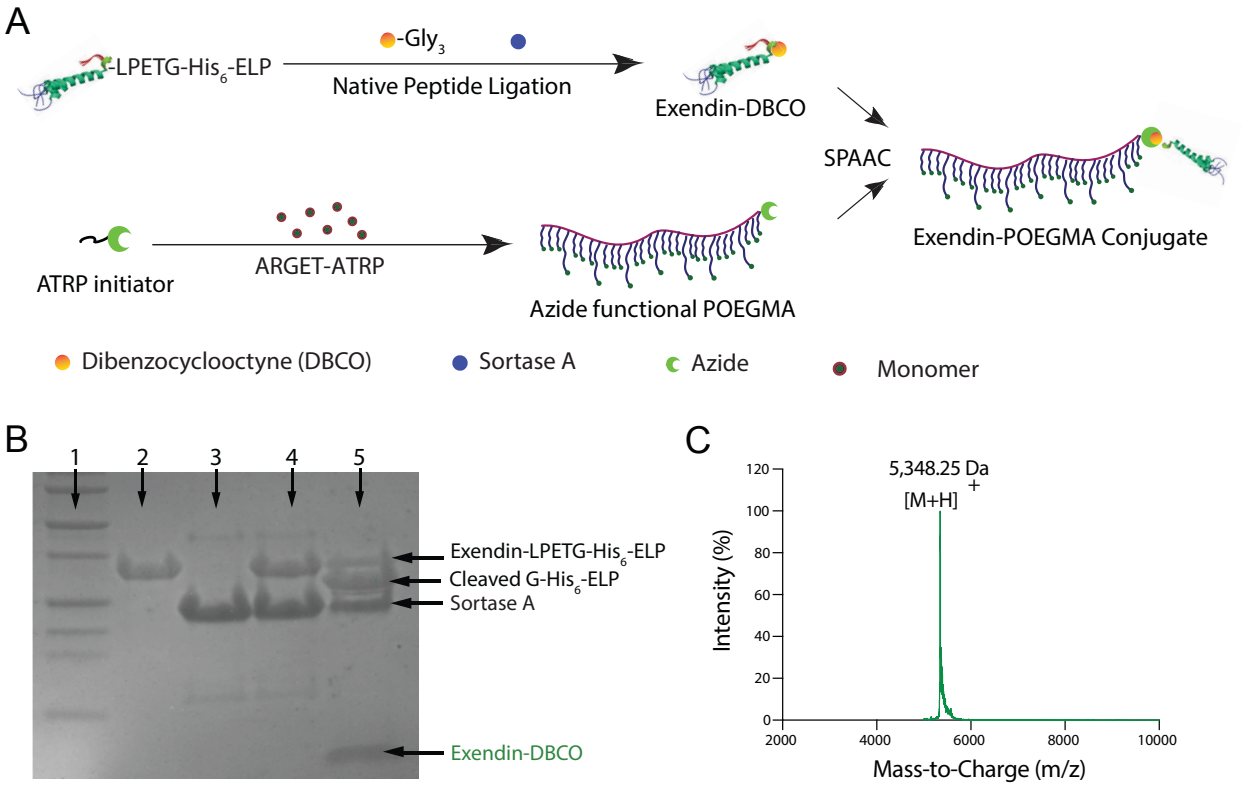

Supplementary Figure 11. Synthesis of site-specific and stoichiometric exendin-POEGMA conjugates. (A) Overview of site-specific and stoichiometric Ex-POEGMA conjugation approach. The bio-orthogonal DBCO group is installed on the C-terminus of exendin by sortase-A mediated native peptide ligation. Sortase A recognizes the LPETG sequence in the exendin-LPETG-His_6-ELP fusion, where ELP is an elastin-like polypeptide, and catalyzes a transpeptidation reaction using DBCO-terminated triglycine, yielding exendin-DBCO. A bio-orthogonal azide group is installed on POEGMA using an azide functional polymerization initiator in ARGET-ATRP. Strain-promoted azide-alkyne cycloaddition is then used to synthesize exendin-POEGMA conjugates. **(B)** Coomassie-stained SDS-PAGE analysis of DBCO conjugation to exendin by sortase A. Lane 1: M_w ladder; lane 2: exendin-LPETG-His_6-ELP; lane 3: sortase A; lane 4: reaction mixture immediately after mixing exendin-LPETG-His_6-ELP with sortase A; lane 5: reaction mixture after 18 h of reaction. **(C)** Exendin-DBCO was analyzed by MALDI-TOF-MS in the positive ion mode. Sinapinic acid was used as the matrix, and insulin and aldolase were used as standards for MALDI-TOF-MS. The major peak at 5,348.25 Da was assigned to the $[M+H]^+$ ion based on the theoretical mass (M) of exendin-DBCO of 5,347.47 Da.

Characterization of exendin-POEGMA conjugates with varied T_t and near-constant M_w.

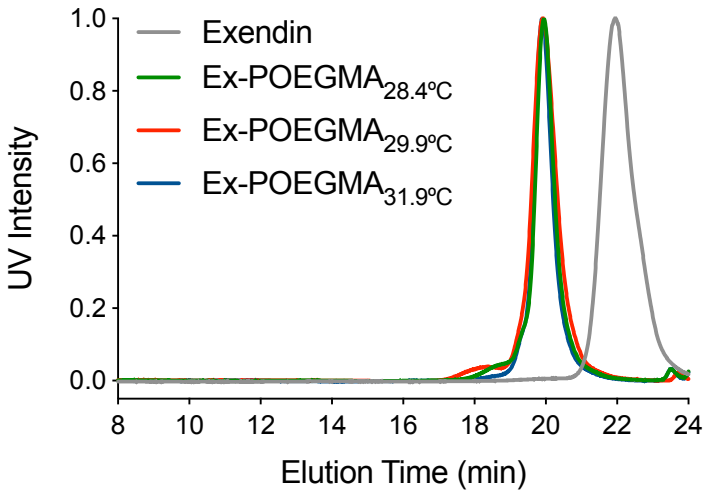

Supplementary Figure 12. SEC traces of exendin-POEGMA conjugates with varied T_t and near-constant M_w. The conjugates were separated by HPLC on a SEC column.

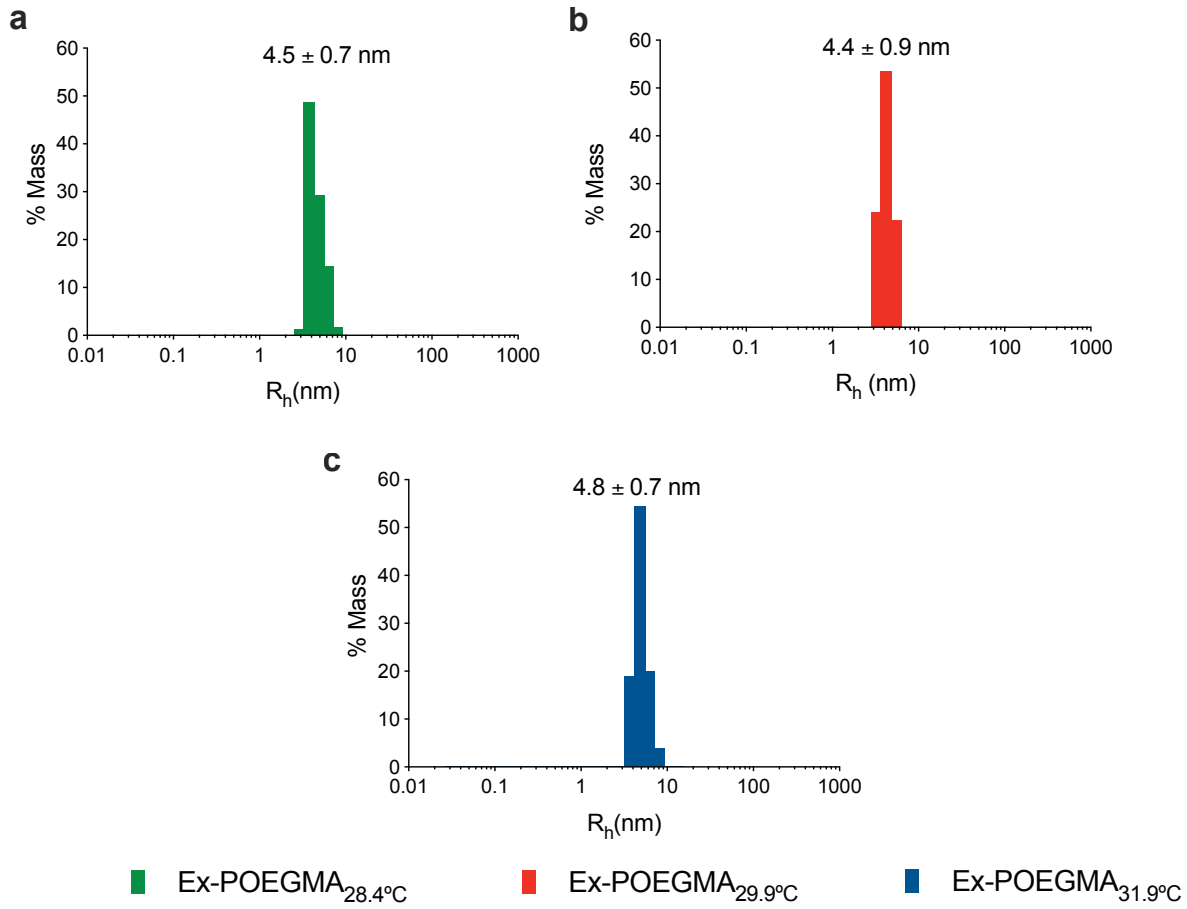

126

127 **Supplementary Figure 13. The R_h of exendin-POEGMA conjugates with varied T_t and near-constant M_w.** The R_h of **(A)** Ex-

128 POEGMA$_{28.4°C}$, **(B)** Ex-POEGMA$_{29.9°C}$, **(C)** Ex-POEGMA$_{31.9°C}$ was characterized by DLS on a temperature-controlled DynaPro Plate

129 Reader (Wyatt Technologies).

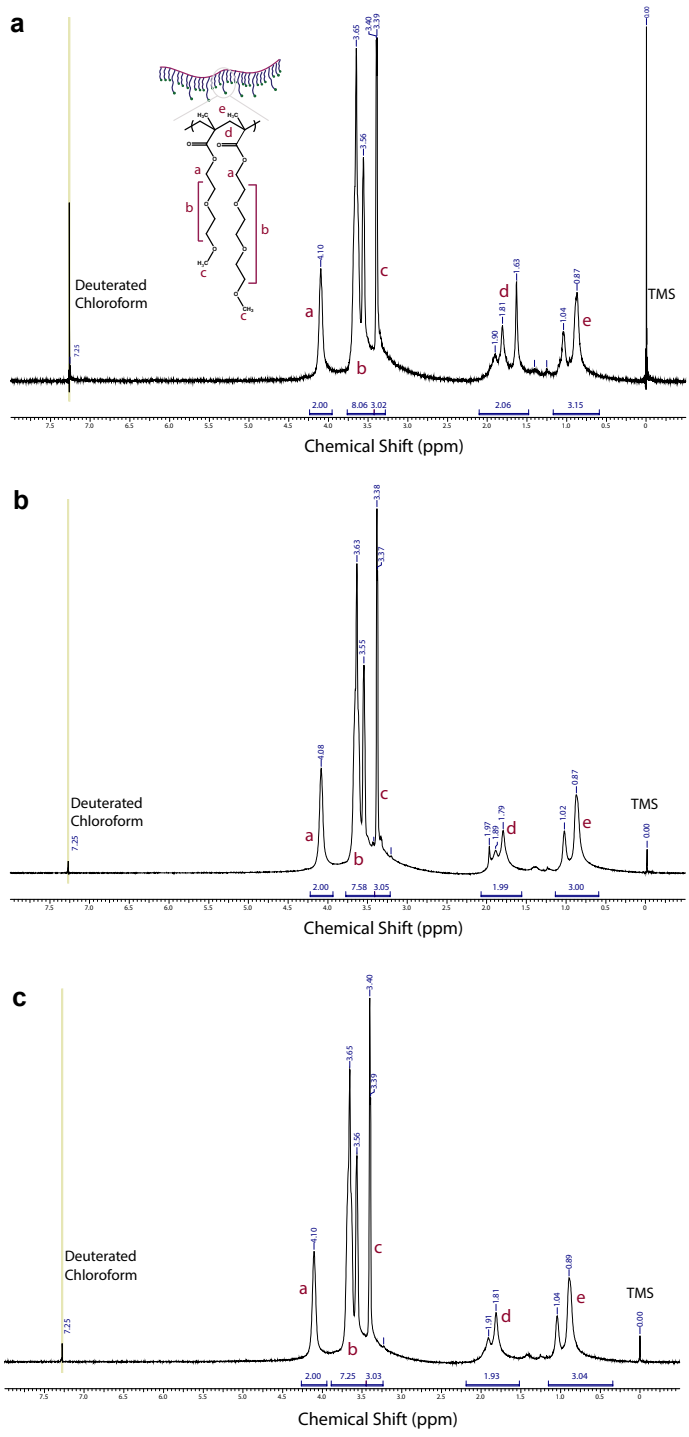

130

131 **Supplementary Figure 14. NMR spectra of POEGMAs used to synthesize Ex-POEGMA conjugates with varied T_t and near-**
132 **constant M_w.** Structure of POEGMAs used to synthesize **(A)** Ex-POEGMA$_{31.9ºC}$, **(B)** Ex-POEGMA$_{29.9ºC}$, and **(C)** Ex-POEGMA$_{28.4ºC}$. Data
133 were acquired using a 400 MHz Varian Inova spectrometer using deuterated chloroform as a solvent and TMS as a reference.
134 Data were analyzed using ACD/NMR software (ACD Labs).

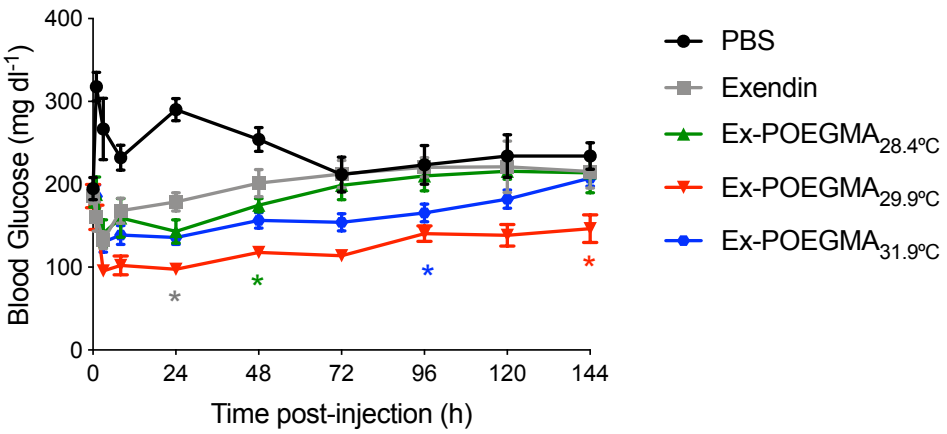

Supplementary Figure 15. Raw fed blood glucose of mice treated with Ex-POEGMA conjugates with similar M_w but varied T_t. Fed blood glucose was monitored after treating 11-week-old male DIO C57BL/6J mice (n=6) with a single *s.c.* injection of Ex-POEGMA conjugates with similar M_w but varied T_t. Data were analyzed by two-way repeated-measures ANOVA followed by *post hoc* Dunnett's multiple comparison test. *The last time point that blood glucose for treatment is significantly lower than that of PBS treated mice. Data showed the mean ± SEM and was considered statistically significant when $p<0.05$.

Characterization of exendin-POEGMA conjugates with optimal T_t and varying M_w.

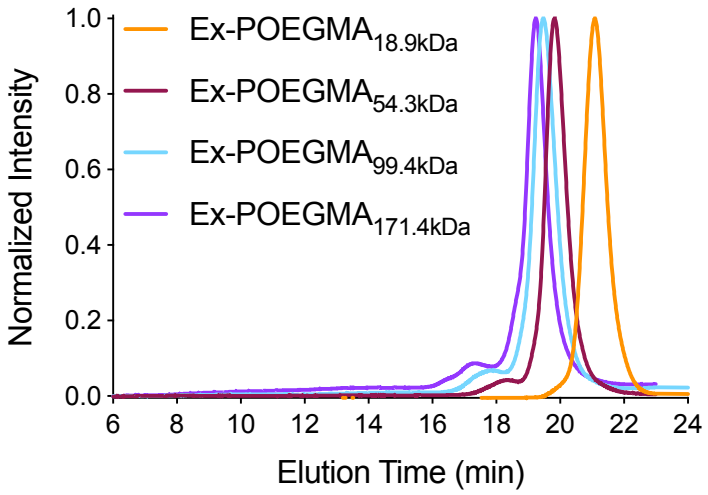

Supplementary Figure 16. SEC traces of Ex-POEGMA conjugates with optimal T_t and varying M_w. The conjugates were separated by HPLC on a SEC column.

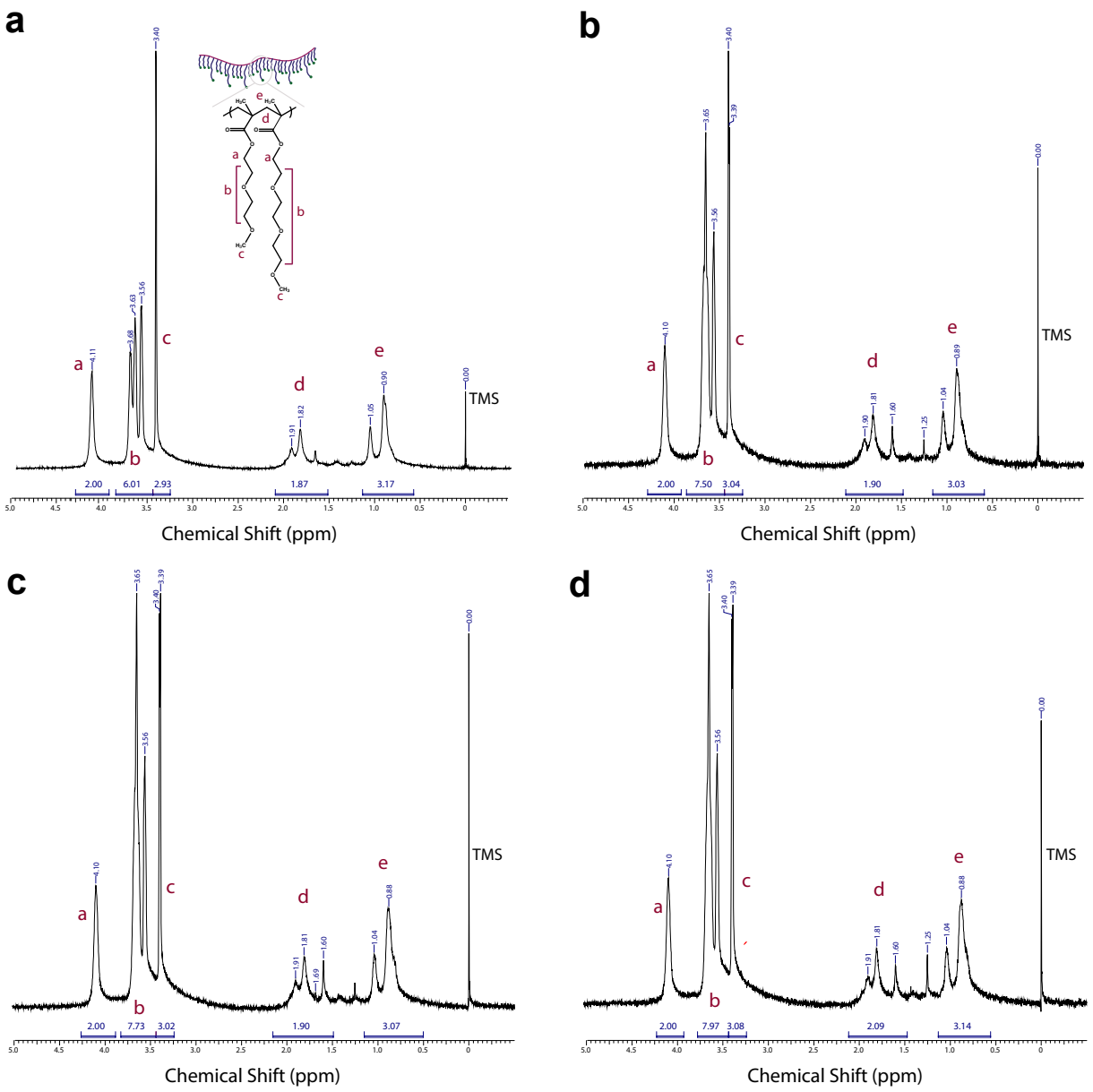

Supplementary Figure 17. NMR spectra of POEGMAs used in the synthesis of Ex-POEGMA conjugates with optimal T_t and varying M_w. Structure of POEGMAs used to synthesize **(A)** Ex-POEGMA$_{18.9kDa}$, **(B)** Ex-POEGMA$_{54.3kDa}$, **(C)** Ex-POEGMA$_{99.4kDa}$, and **(D)** Ex-POEGMA$_{171.4kDa}$. Data were acquired using a 400 MHz Varian Inova spectrometer using deuterated chloroform as a solvent and TMS as a reference. Data were analyzed using ACD/NMR software (ACD Labs).

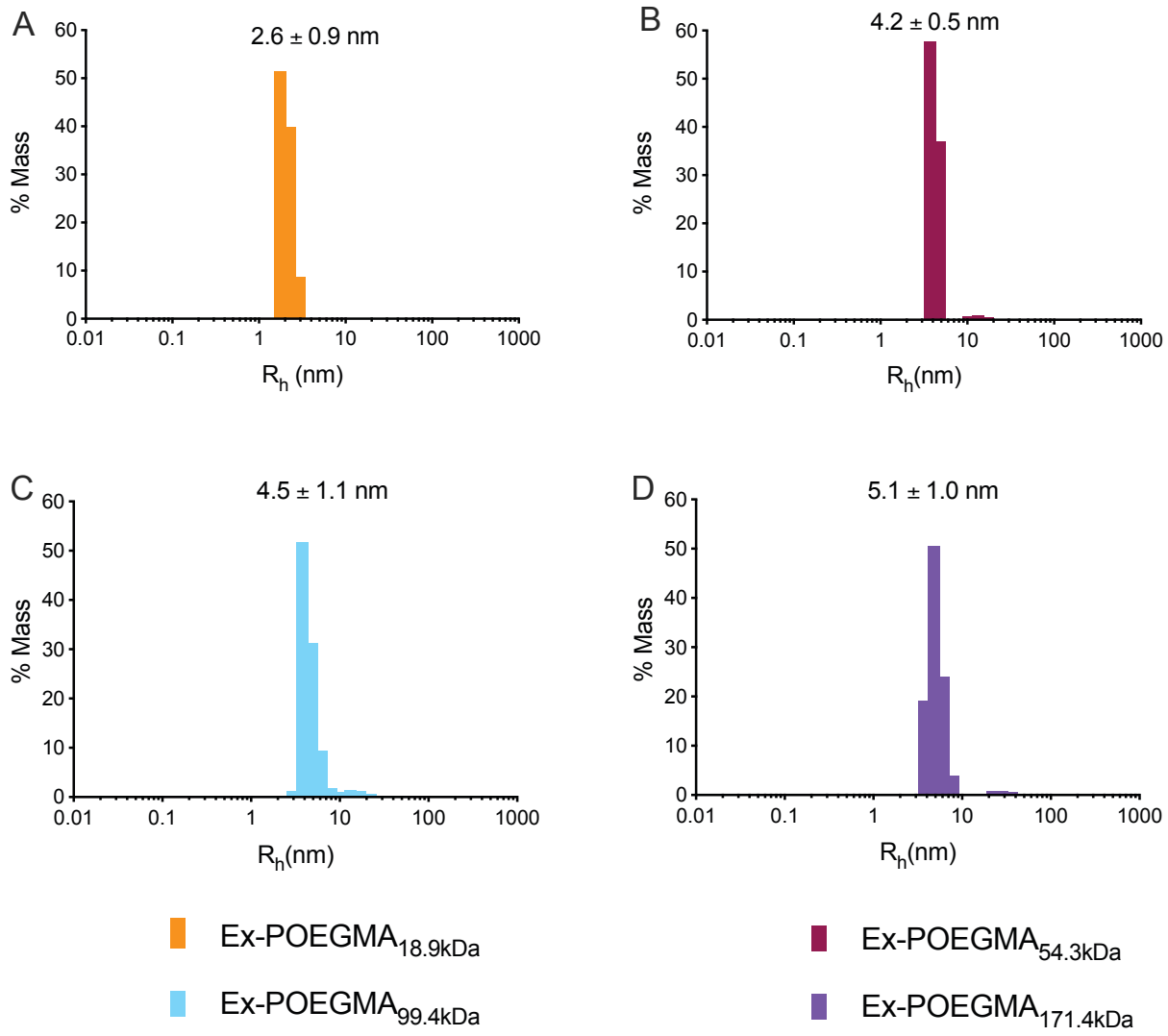

150

151 **Supplementary Figure 18.** ***The R_h of Ex-POEGMA conjugates with*** **optimal T_t and varying M_w.** The Rh of **(A)** Ex-POEGMA$_{18.9kDa}$,

152 **(B)** Ex-POEGMA$_{54.3kDa}$, **(C)** Ex-POEGMA$_{99.4kDa}$, and **(D)** Ex-POEGMA$_{171.4kDa}$ was characterized by DLS on a temperature-controlled

153 DynaPro Plate Reader (Wyatt Technologies).

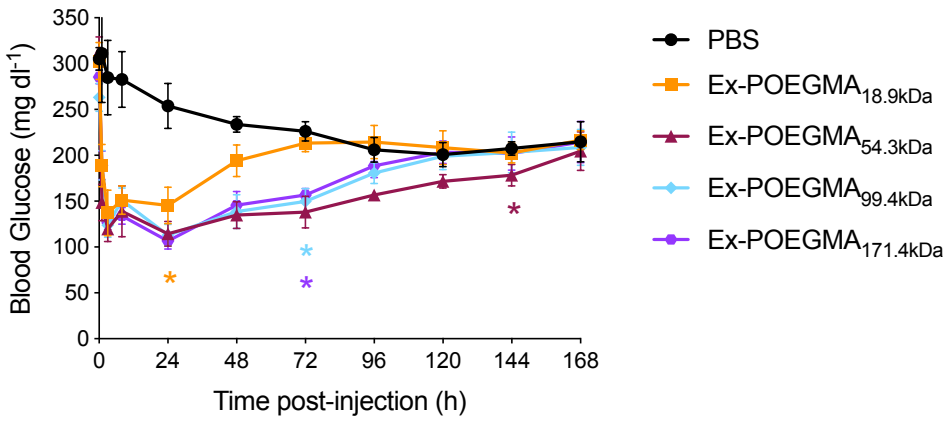

154

155 **Supplementary Figure 19. Raw fed blood glucose of mice treated with Ex-POEGMA conjugates with varying M_w but optimal**
156 **T_t.** Fed blood glucose was monitored after treating 11-week-old male DIO C57BL/6J mice (*n*=6) with a single *s.c.* injection of Ex-
157 POEGMA conjugates. Data were analyzed by two-way repeated-measures ANOVA followed by *post hoc* Dunnett's multiple
158 comparison test. *The last time point that blood glucose for treatment is significantly lower than that of PBS treated mice. Data
159 showed the mean ± SEM and was considered statistically significant when $p<0.05$.

160 *Dose optimization of Ex-POEGMA$_{opt}$.* In the dose optimization study, varied doses of Ex-POEGMA$_{opt}$ were
161 injected *s.c* into 11-week-old male DIO C57BL6/J mice (*n*=5) that were kept on a 60 kilocalorie % fat diet
162 for five weeks before the study. Th injection concentration (500 µM) and volume (120 µl) were kept
163 constant across groups to prevent differences in T_t by keeping the volume of lower dose injections the
164 same as that of the highest dose by adding free POEGMA to make up the difference in volume (500
165 µM). The fed blood glucose level and body weight (data not shown) were measured at 1-, 4-, 8-, 24-, 48-,
166 72-, 96-, 120-, 144- and 168 h post-injection, as described in the Methods. Larger injection doses of the
167 conjugate resulted in more extended blood glucose control. Because an injection dose of 1500 nmol kg^{-1}
168 did not provide any additional benefit, 1000 nmol kg^{-1} was chosen as the optimal injection dose.

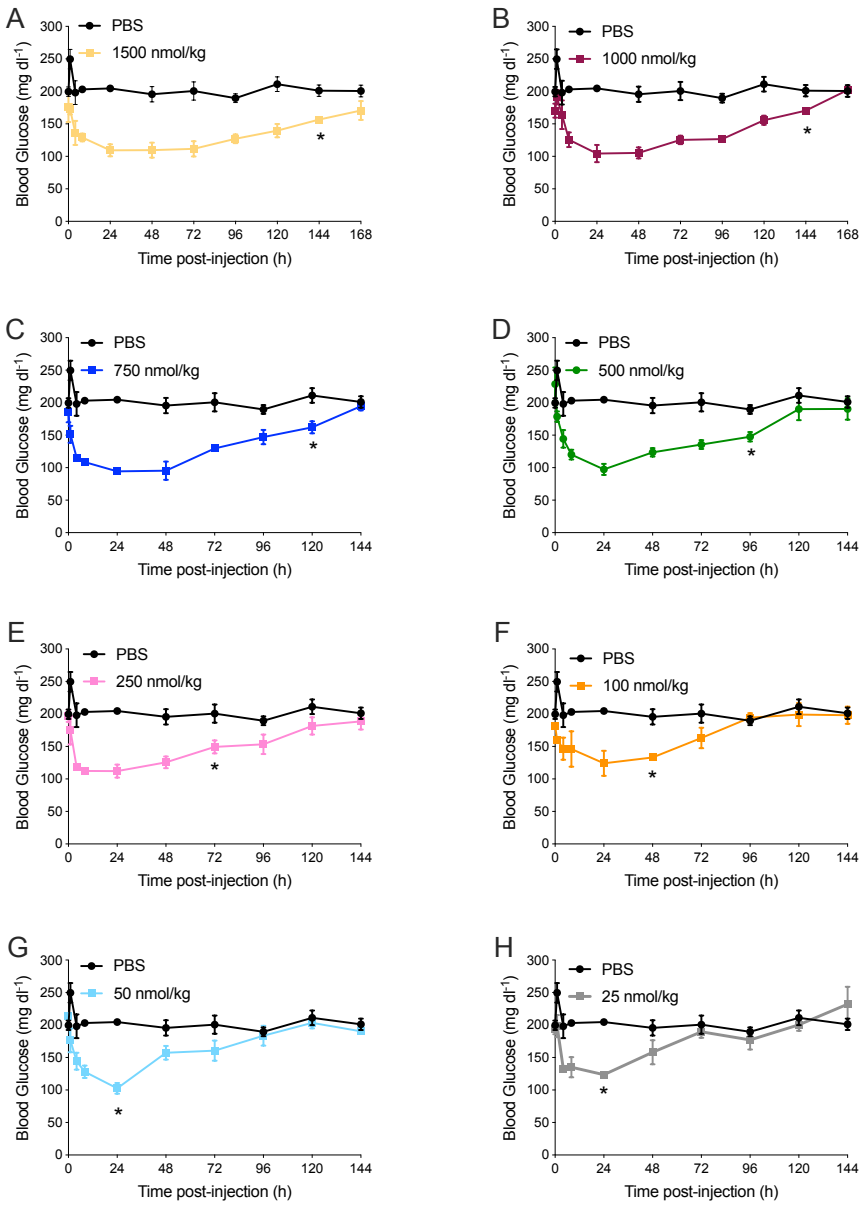

Supplementary Figure 20. Dose optimization of Ex-POEGMA$_{opt}$. **(A)** 1500, **(B)** 1000, **(C)** 750, **(D)** 500, **(E)** 250, **(F)** 100, **(G)** 50, and **(H)** 25 nmol kg^{-1} bodyweight doses of Ex-POEGMA$_{opt}$ were injected *s.c.* into 11-week-old male DIO C57BL6/J mice (n=5). Fed blood glucose levels was measured at 1-, 4-, 8-, 24-, 48-, 72-, 96-, 120-, 144- and 168 h post-injection, as described in the Methods. Data were analyzed by two-way repeated-measures ANOVA followed by *post hoc* Dunnett's multiple comparison test. *The last time point that blood glucose for treatment is significantly lower than that of PBS treated mice. Data showed the mean ± SEM and was considered statistically significant when p<0.05.

Characterization of PEG and POEGMA conjugates of exendin

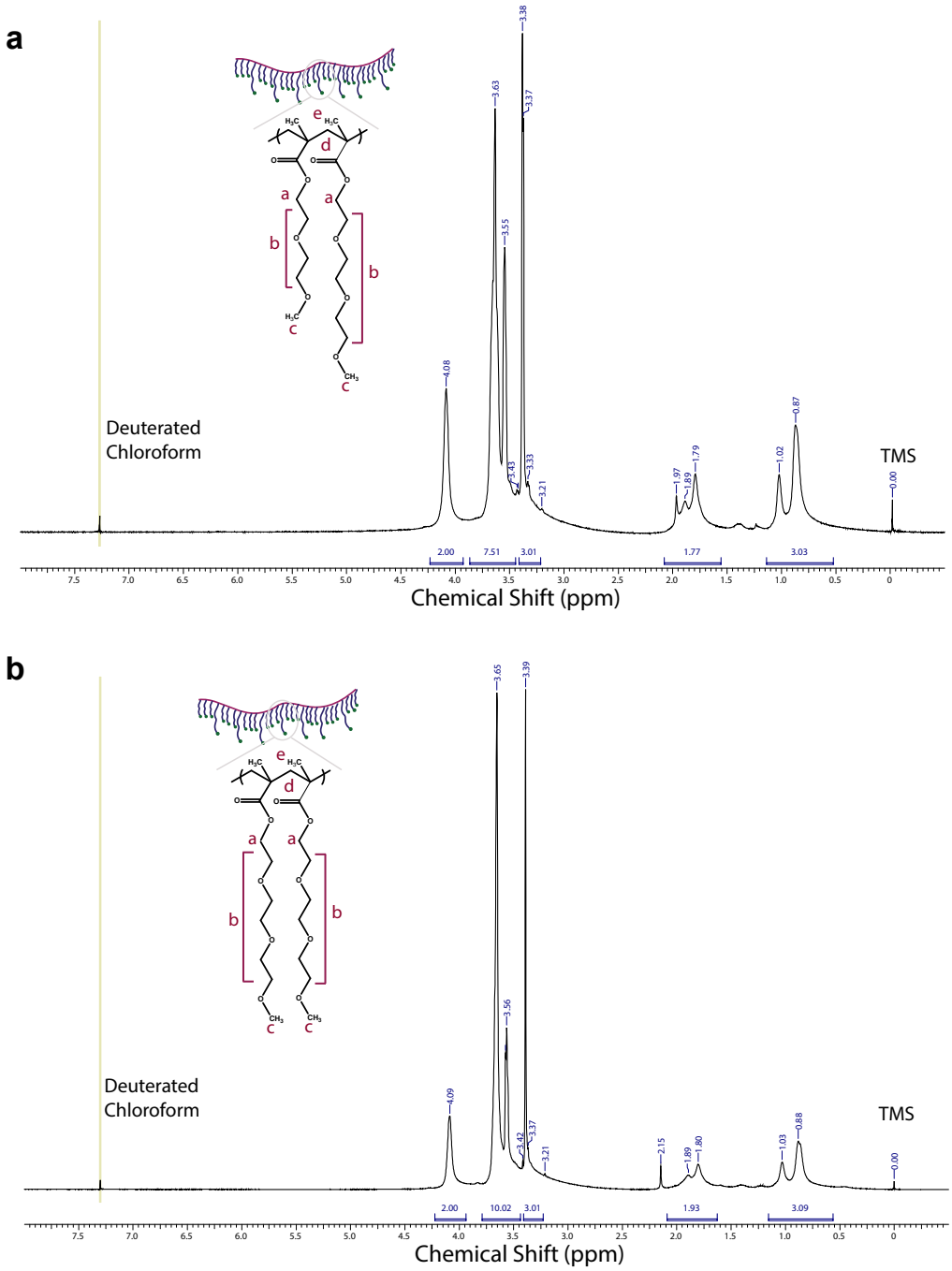

Supplementary Figure 21. NMR spectra of POEGMAs used for the synthesis of the depot-forming and soluble exendin-POEGMA conjugates. Structural analysis of POEGMAs used in the synthesis of **(A)** Ex-POEGMA$_{opt}$ and **(B)** Ex-POEGMA$_{sol}$. Data were acquired using a 400 MHz Varian Inova spectrometer using deuterated chloroform as a solvent and TMS as a reference. Data were analyzed using ACD/NMR software (ACD Labs).

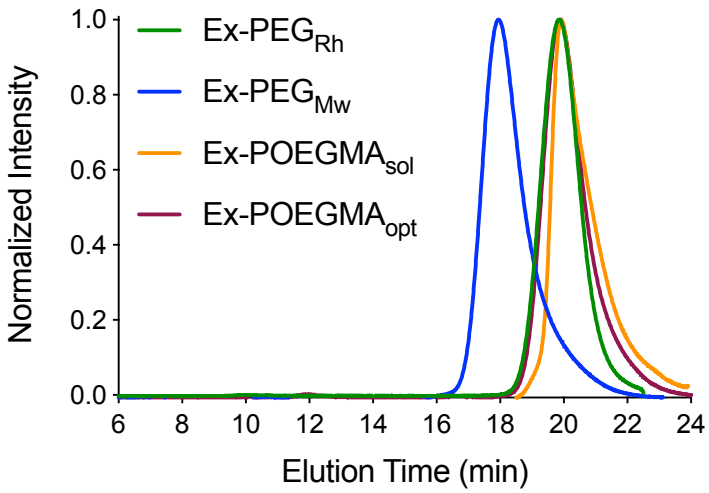

182

183 **Supplementary Figure 22. SEC traces of PEG and POEGMA conjugates of exendin.** The conjugates were separated by HPLC on a

184 SEC column.

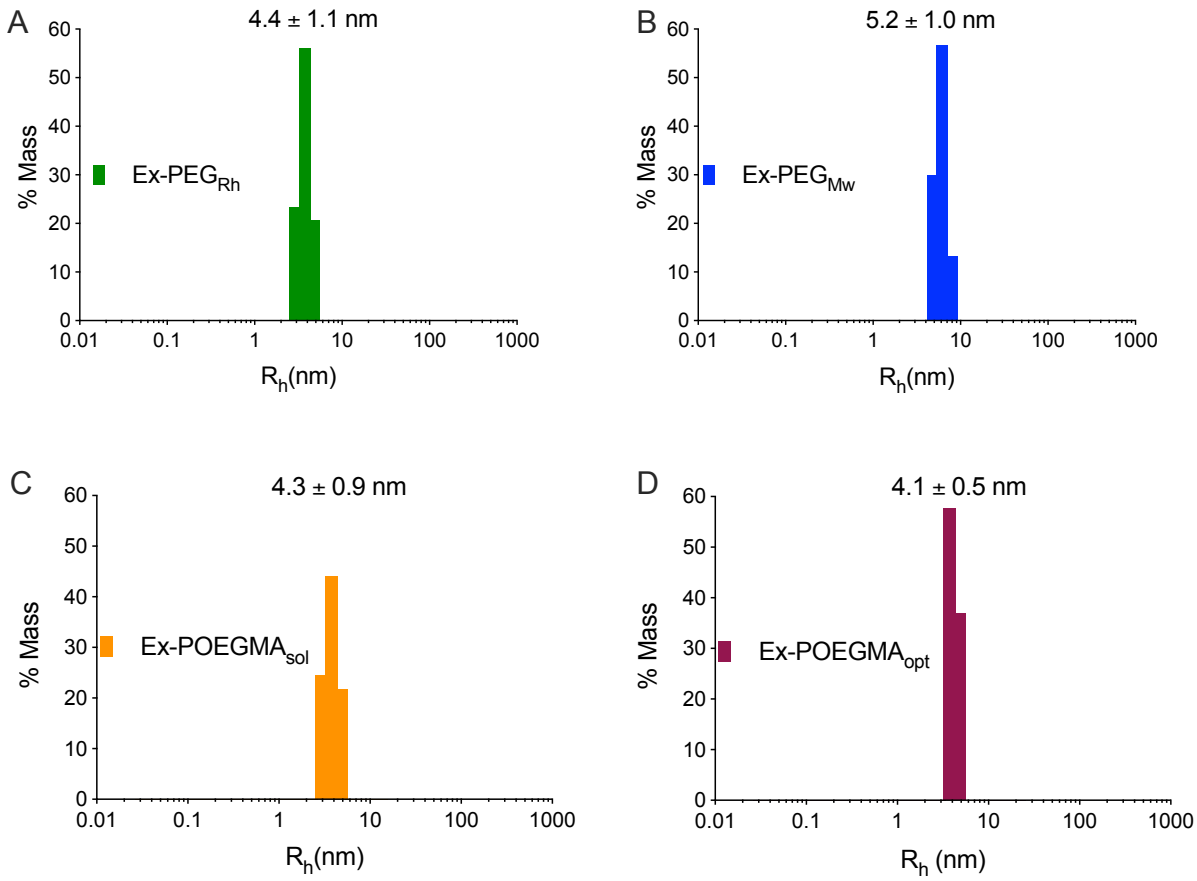

185

186 **Supplementary Figure 23. The R_h of PEG and POEGMA conjugates of exendin.** The R_h of **(A)** Ex-PEG$_{Rh}$, **(B)** Ex-PEG$_{Mw}$, **(C)** Ex-

187 POEGMA$_{sol}$, and **(D)** Ex-POEGMA$_{opt}$ was characterized by DLS on a temperature-controlled DynaPro Plate Reader (Wyatt

188 Technologies).

Section 3. Short-term pharmacokinetics and pharmacodynamics

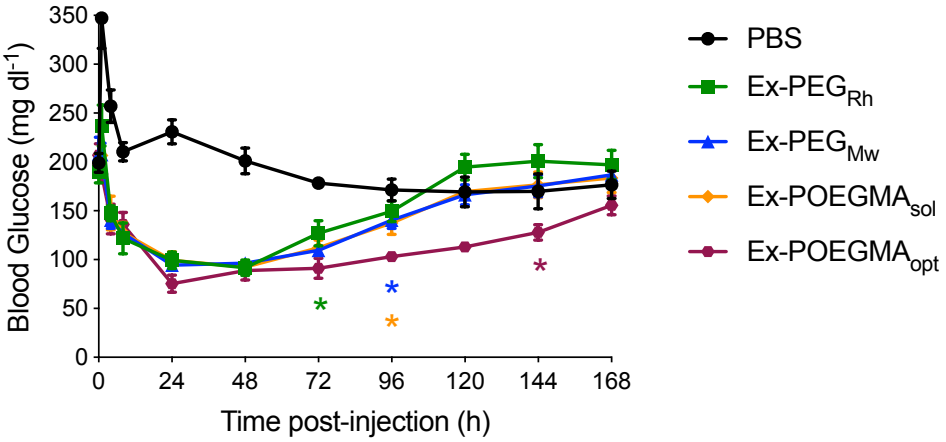

Supplementary Figure 24. Raw fed blood glucose of mice treated with the depot-forming Ex-POEGMA$_{opt}$ and its soluble POEGMA and PEG counterparts. Fed blood glucose was monitored after treating 11-week-old male DIO C57BL/6J mice (*n*=6) with a single *s.c.* injection of Ex-POEGMA$_{opt}$, Ex-POEGMA$_{sol}$, Ex-PEG$_{Rh}$, and Ex-PEG$_{Mw}$. Data were analyzed by two-way ANOVA followed by *post hoc* Dunnett's multiple comparison test. *The last time point that blood glucose for treatment is significantly lower than that of PBS treated mice. Data showed the mean ± SEM and was considered statistically significant when $p<0.05$.

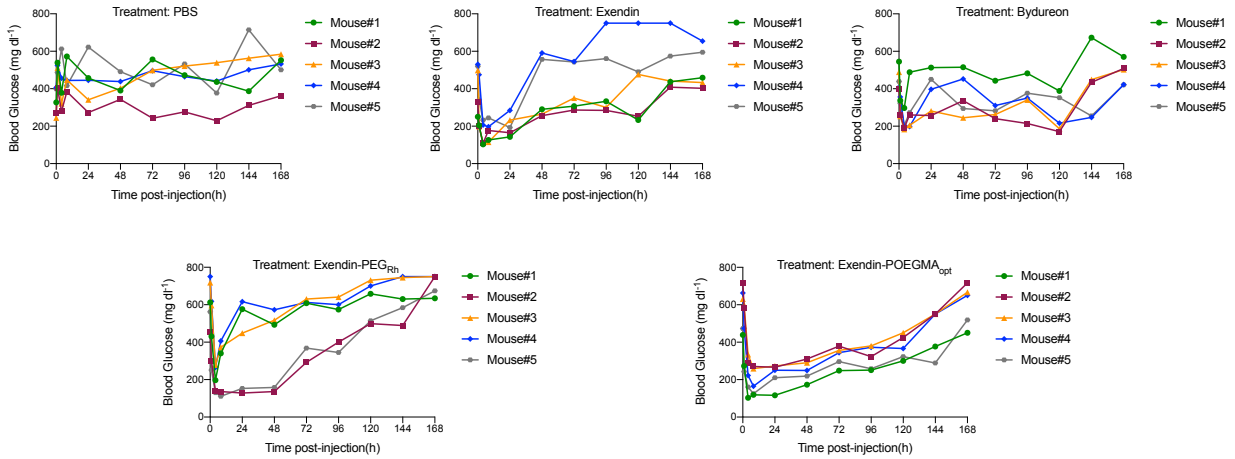

196

197 **Supplementary Figure 25. Individually plotted raw fed blood glucose of short-term-treated *db/db* mice.** 6-week-old *db/db* mice

198 (*n*=5) received a single *s.c.* injection of **(A)** PBS, **(B)** exendin, **(C)** Bydureon, **(D)** Ex-PEG$_{Rh}$, and **(E)** Ex-POEGMA$_{opt}$. Fed blood glucose

199 was measured as described in the Methods.

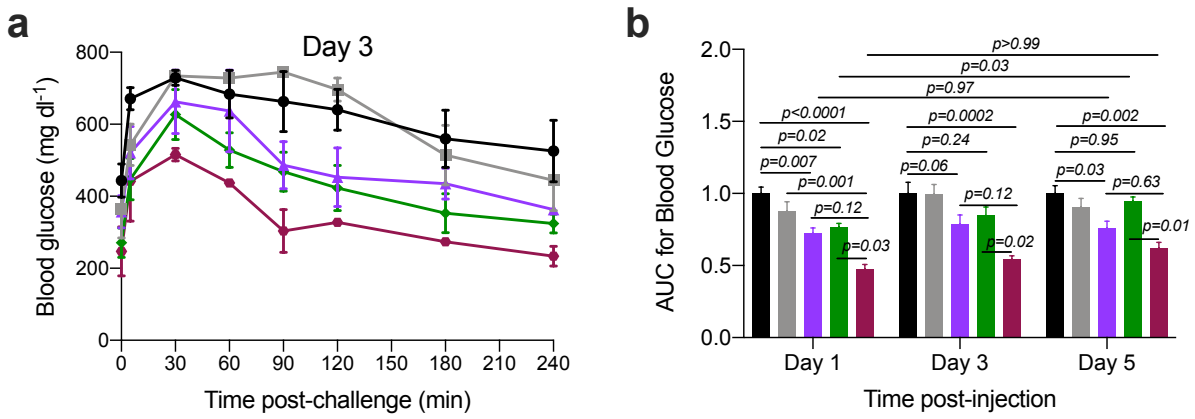

Supplementary Figure 26. Ex-POEGMA$_{opt}$ outperforms its PEG counterpart and a clinical sustained-release exendin formulation, Bydureon, in providing glycemic control. An *i.p.* glucose challenge was performed at **(A)** day 1, **(B)** day 3, and **(C)** day 5 post-injection of treatments. 1500 g per kg body weight glucose was administered *s.c.* into 6-week-old *db/db* mice (n=5), followed by monitoring their blood glucose. **(B)** AUC of blood glucose was quantified and is reported by the day it was measured after administration of the drug. Data represent the mean and standard error of the mean (SEM). Data were analyzed by two-way repeated-measures ANOVA, followed by *post-hoc* Tukey's multiple comparison test. Data were considered statistically significant when p<0.05.

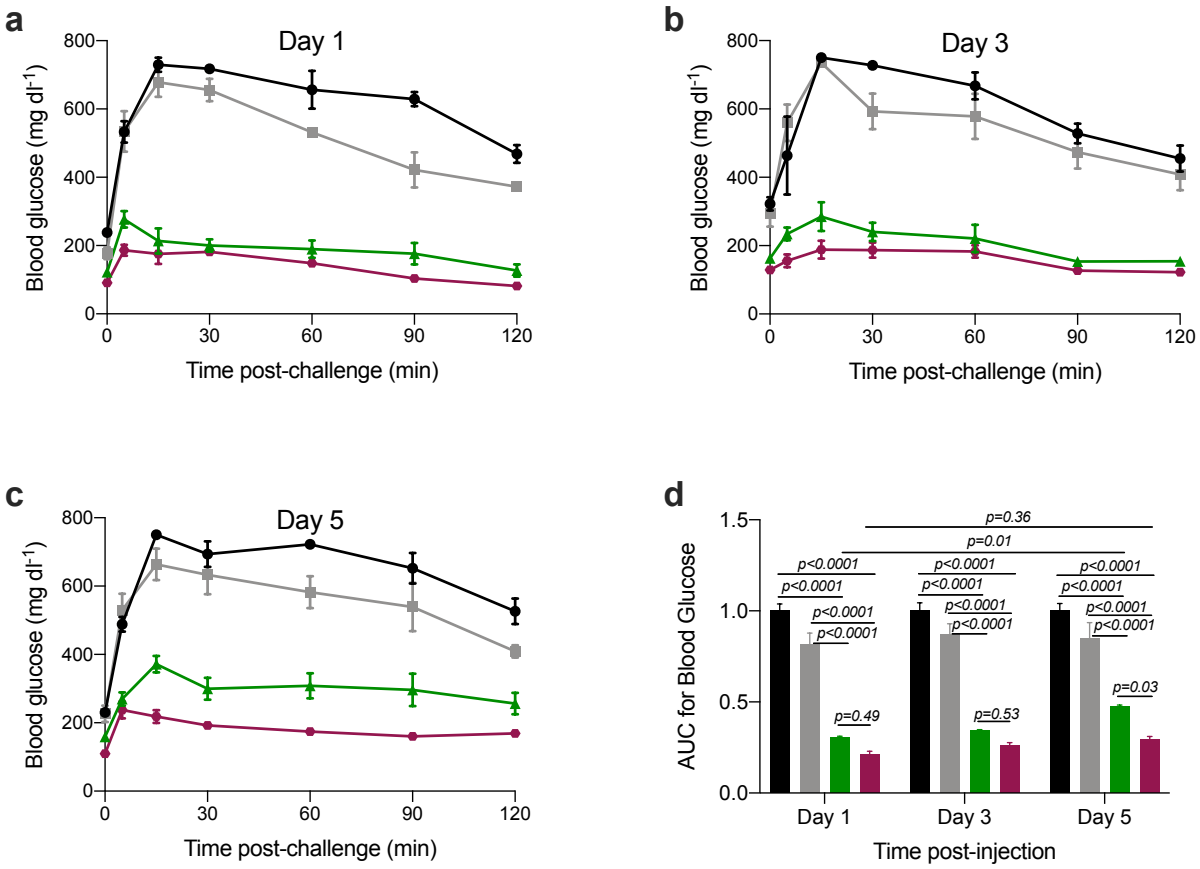

208

209

210 **Supplementary Figure 27. Ex-POEGMA$_{opt}$ outperforms its PEG counterpart in providing glycemic control.** An *i.p.* glucose
211 challenge was performed at **(A)** day 1, **(B)** day 3, and **(C)** day 5 post-injection of treatments. 1500 g per kg body weight glucose
212 was administered to 11-week-old male DIO C57BL/6J mice (n=5), followed by monitoring their blood glucose. **(D)** AUC of blood
213 glucose was quantified as reported by the day it was measured after drug administration. Data represent the mean ± SEM. Data
214 were analyzed by two-way repeated-measures ANOVA, followed by *post-hoc* Tukey's multiple comparison test. Data were
215 considered statistically significant when p<0.05.

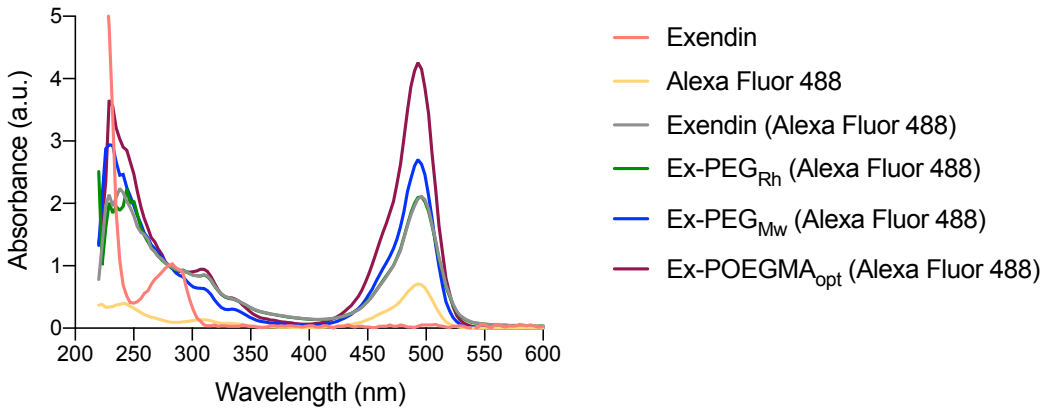

Supplementary Figure 28. UV-vis absorbance spectrum of fluorescently labeled treatments used in the pharmacokinetics experiment. Exendin variants were reacted with an amine-functionalized Alexa Fluor 488, followed by purification of the conjugate by gel filtration. UV-vis absorbance spectra of the fluorophore conjugate of the exendin variants were measured on a Nanodrop spectrometer using unmodified exendin as a negative control and Alexa Fluor 488 as a positive control.

Section 4. Long-term efficacy

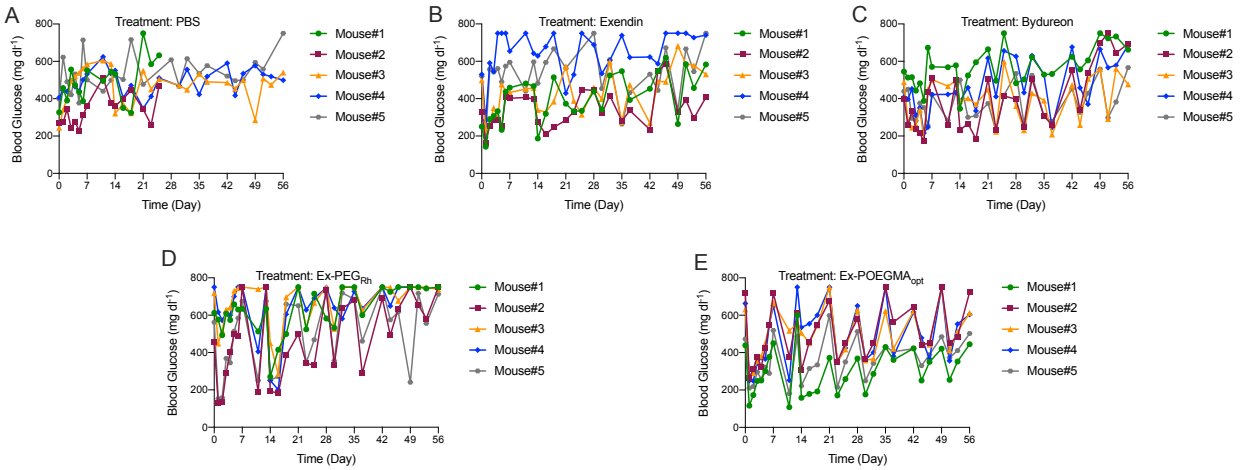

Supplementary Figure 29. Individually plotted raw fed blood glucose of long-term-treated *db/db* mice. 6-week-old *db/db* mice (*n*=5) received weekly *s.c.* injections of **(A)** PBS, **(B)** exendin, **(C)** Bydureon, **(D)** Ex-PEG$_{Rh}$, and **(E)** Ex-POEGMA$_{opt}$ for eight weeks. Fed blood glucose was measured as described in the Methods. Mice #1 and #2 in the PBS group died due to cage flooding on Day 28. Mouse#4 in the Ex-PEG$_{Rh}$ group was found dead on Day 51.

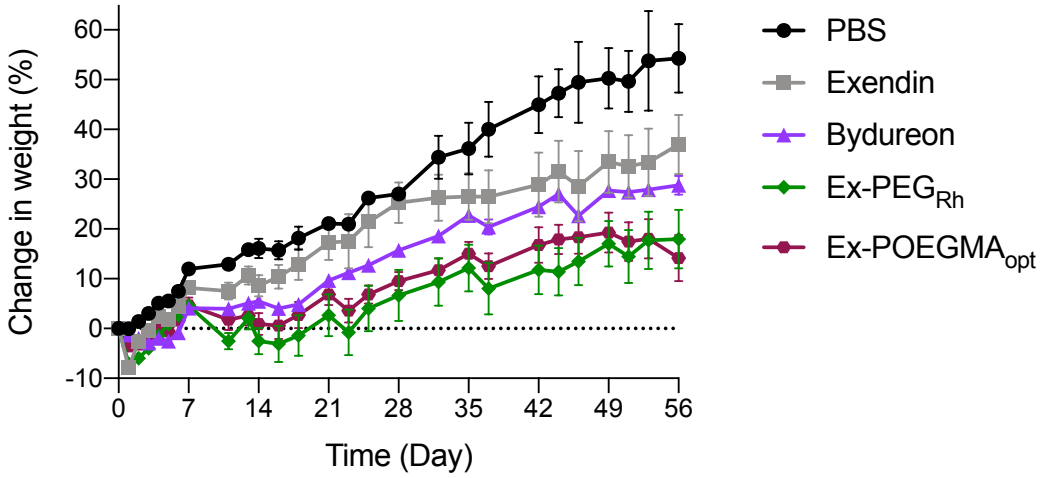

227

228 **Supplementary Figure 30. Change in body weight of long-term-treated *db/db* mice.** 6-week-old *db/db* mice (*n*=5) received

229 weekly *s.c.* injections of PBS, exendin, Bydureon, Ex-PEG$_{Rh}$, and Ex-POEGMA$_{opt}$ for eight weeks. Weight was tracked every other

230 day.

Section 5. Immunogenicity

Design, optimization, and validation of a Luminex multiplexed immunoassay (LMI).

Assay Design. We designed an assay to assess the titer, specificity (anti-protein/peptide, anti-PEG, or anti-POEGMA), and subtype (IgM or IgG) of ADAs using a LMI platform. The LMI platform uses drug or drug-polymer conjugates that are covalently coupled to fluorescently barcoded magnetic beads to capture ADAs. We conjugated exendin, exendin-PEG, and exendin-POEGMA and their OVA counterparts—OVA, OVA-PEG, OVA-POEGMA—to different sets of fluorescently barcoded magnetic beads. This bead design allowed us to determine the specificity of the ADAs, such that if exendin-PEG-treated mice plasma results in a positive signal for the exendin-PEG- and OVA-PEG-conjugated bead sets but not for the exendin-conjugated bead set, that would give a clear indication that the ADAs are PEG-specific and not protein specific.

Drug synthesis, purification, and characterization for bead coupling. Due to the steric effects of high M_w POEGMA and PEG used in the optimal conjugate synthesis on the bead coupling efficiency, we synthesized exendin and OVA conjugates of PEG and POEGMA for bead coupling using polymers with an M_w of ~10 kDa, yielding exendin-PEG_{10K}, exendin-$POEGMA_{10K}$, OVA-PEG_{10K}, and OVA-$POEGMA_{10K}$. Exendin-PEG_{10K} and exendin-$POEGMA_{10K}$ conjugates were synthesized, purified, and characterized, as described in Methods with minor modifications. Briefly, azide functional, linear PEG was purchased from Creative PEGWorks. Azide functional POEGMA was synthesized by reacting the EG3 monomer (2.5 mmol; 565.4 µL), the catalytic complex (0.1 mmol TPMA and 0.01 mmol $CuBr_2$; 62.5 µL), the polymerization initiator (62.5 µL in methanol; 0.01 mmol) in a mixture of methanol (1437.5 µL) and 100 mM NaCl (4432.8 µL) for 2 hours. Exendin-PEG_{10K} and exendin-$POEGMA_{10K}$ conjugates were analyzed for M_n, M_w, and $Đ$ using SEC-MALS **(Supplementary Fig. 31a; Supplementary Table 2)**.

OVA conjugates of PEG and POEGMA were synthesized via activated carbonate-amine conjugation. Nitrophenyl-carbonate (NPC) functional PEG was purchased from Creative PEGWorks. A hydroxyl functional POEGMA was synthesized by reacting EG3 (10 mmol; 2261.6 µL), the catalytic complex (0.08 mmol TPMA and 0.01 mmol $CuBr_2$; 100 µL), 2-Hydroxyethyl 2-bromoisobutyrate (Sigma) (200 µL in methanol; 0.04 mmol) in a mixture of methanol (5.800 mL) and 100 mM NaCl (11.638 mL) for 1.5 h. The resulting hydroxyl-functional POEGMA (5 mM in DCM) was reacted with p-nitrophenyl carbonate (100 mM in DCM) in the presence of pyridine (240 mM in DCM) for 16 h to convert the hydroxyl end-group to an NPC. The resulting NPC-functional POEGMA was purified via filtration followed by diethyl ether precipitation. NPC functionalization yield was 79.7%, calculated by nuclear magnetic resonance (NMR) spectroscopy. NPC functional POEGMA and PEG were reacted with OVA (Invivogen; 2 mg ml^{-1}) at a 10: 1 molar ratio for 5 h in 200 mM phosphate buffer at pH 8, yielding OVA-PEG_{10K} and OVA-$POEGMA_{10K}$ conjugates. The resulting conjugates were purified by anion exchange chromatography to > 98% purity using 20 mM sodium phosphate buffer at pH 8.6 with a NaCl gradient of 0-50% and were then desalted and lyophilized. The conjugates were analyzed for M_n, M_w, and $Đ$ using SEC-MALS **(Supplementary Fig. 31b; Supplementary Table 2)**.

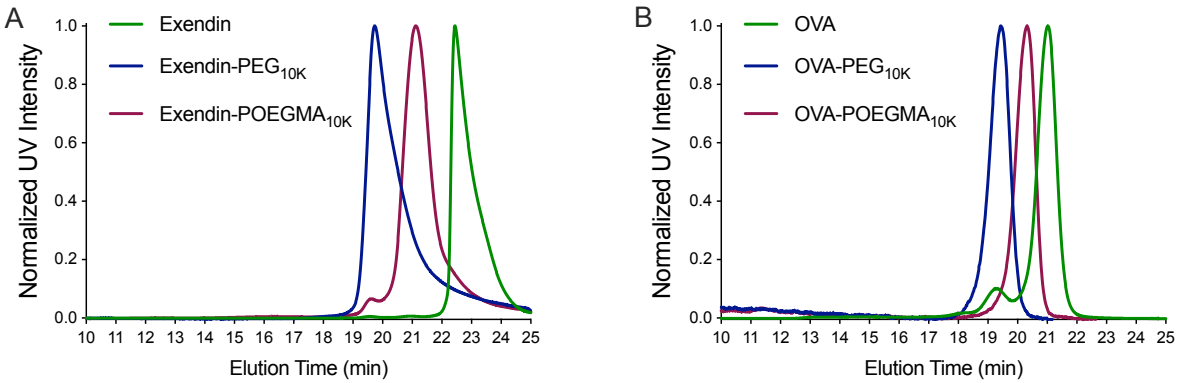

Supplementary Figure 31. SEC traces of the drugs used for the bead coupling. The conjugates were separated on a Shodex KW 803 SEC-HPLC column using 10 mM phosphate buffer (pH.7.2) as a mobile phase. The flow rate was 0.5 ml min^{-1}.

Supplementary Table 2. Characterization of drugs used in bead coupling. M_w and $Đ$ values were determined by SEC-MALS. The data summarized here is shown in Supplementary Figure 32. Subscript shows the M_w of the polymer used in the synthesis of the conjugate. Conjugation stoichiometry was defined as the number of polymer chains per peptide or protein and was calculated using ASTRA (Wyatt Technology). The R_h was calculated by DLS and reported as the mean ± standard deviation (n= 10). N/A (Not applicable).

Compound	Polymer M_w (kDa)	Polymer Đ	M_w (kDa)	$Đ$	Conjugation Stoichiometry	R_h (nm)
Exendin	N/A	N/A	4.1	1.00	N/A	2.0 ± 0.7
Exendin-PEG_{10K}	10.2	1.06	16.2	1.10	1.01	3.8 ± 0.2
Exendin-$POEGMA_{10K}$	10.3	1.06	17.3	1.07	1.01	2.7 ± 0.8
OVA	N/A	N/A	42.9	1.00	N/A	2.5 ± 0.6
OVA-PEG_{10K}	10.3	1.01	54.5	1.16	1.03	4.5 ± 0.7
OVA-$POEGMA_{10K}$	10.4	1.09	54.7	1.07	1.03	3.3 ± 0.3

Synthesis and characterization of drug coupled Luminex magnetic beads. The drugs and drug-polymer conjugates —exendin, exendin-PEG_{10K}, exendin-$POEGMA_{10K}$, OVA, OVA-PEG_{10K}, and OVA-$POEGMA_{10K}$— were covalently coupled to different sets of fluorescently barcoded MagPlex magnetic beads (Luminex) via carbodiimide chemistry by following the manufacturer's instructions with minor modifications.[1] The concentration of drug or drug-polymer conjugate used in the coupling reactions were carefully titrated to ensure that the resulting bead sets had equal amounts of antigen per bead, as described below.

To couple exendin (Santa Cruz Biotechnology), exendin-PEG_{10K}, and exendin-$POEGMA_{10K}$, beads were first amine-functionalized as described below. The amine-modified beads were then conjugated to the exendin variants. Briefly, 12.5 million carboxyl-functional beads were rinsed with 0.5 ml of coupling buffer II (0.1 M MES; pH 6.0). Rinsed beads were incubated with 500 µL of adipic acid dihydrazide (ADH) (35 mg ml^{-1}) and 100 µL of EDC (200 mg ml^{-1}) for 1 h. The resulting amine-modified beads were washed and resuspended in 200 µL of the coupling buffer II. 31.8 µL of exendin, 41.7 µL of exendin-PEG and 39.7 µL of exendin-POEGMA solutions (187.8 µM) and 25 µL of EDC (200 mg ml^{-1}) were added to amine-modified beads followed by bringing the final volume to 250 µL and incubation for 2 hours. The resulting drug-coupled beads were blocked overnight in assay buffer, which is 0.2% (w/v) I-Block protein-based

292 blocking reagent (Thermo Scientific) in PBS (Hyclone). The next morning, they were washed three times,
293 resuspended, and counted using a hemocytometer for final concentration.

294 For the OVA, OVA-PEG_{10K}, and OVA-$POEGMA_{10K}$ coupling reaction, 12.5 million beads were rinsed
295 with 250 µL deionized water. Rinsed beads were resuspended in 50 µL activation buffer (0.1 M NaH_2PO_4;
296 pH 6.2), followed by the addition of 25 µL of 100 mg ml^{-1} N-hydroxy sulfosuccinimide (Sulfo-NHS; Thermo
297 Scientific) and 1-Ethyl-3-[3-dimethylaminopropyl] carbodiimide hydrochloride (EDC; Thermo Scientific)
298 and incubation for 20 min. Activated beads were washed with 1 mL coupling buffer (50 mM 2-(N-
299 morpholino) ethanesulfonic acid (MES); pH 5.0) three times and resuspended in 500 µL of the coupling
300 buffer. 93.7 µL of OVA, 106.6 µL of OVA-PEG_{10K}, and 105.6 µL of OVA-$POEGMA_{10K}$ solutions (46.8 µM) were
301 transferred, followed by bringing the total volume to 1 ml with the coupling buffer and incubation for 2
302 h. The resulting drug-coupled beads were blocked overnight in the assay buffer, washed three times,
303 resuspended, and counted using a hemocytometer. This protocol was also used to couple mouse IgG
304 (Abcam; 2.5 µL; 2 mg ml^{-1}) and IgM (Bio-Rad; 6.25 µL; 2 mg ml^{-1}) as positive controls.

305 The resulting beads were characterized for their level of drug conjugation using anti-drug
306 antibodies at varied concentrations by following the manufacturer's instructions. Briefly, 50 µl of each set
307 of beads (50,000 bead ml^{-1} in the assay buffer) was transferred to a black, round-bottom 96-well-plate
308 (Corning). Next, serial dilutions were prepared of mouse anti-OVA IgG (Abcam #17293) mouse anti-
309 exendin IgG (Abcam #23407), mouse anti-PEG IgG (Abcam #195350), R-Phycoerythrin-conjugated goat
310 anti-mouse IgG (Jackson Immunoresearch; 115-115-164), and biotinylated goat anti-mouse IgM (Jackson
311 Immunoresearch; 115-065-075) in assay buffer. 50 µL of the resulting solutions were transferred to wells
312 followed by incubation for 1 h on an orbital shaker. After incubation, a 96-well-plate was placed on a
313 magnetic ring stand (Invitrogen) and incubated for 60 s for capture of the magnetic particles to occur. The
314 supernatant was discarded, and wells were washed with 100 µl of the assay buffer. Drug-coupled beads
315 were incubated with 100µl of 5 µg ml^{-1} R-Phycoerythrin-conjugated goat anti-mouse IgG (Jackson

Immunoresearch; #115-115-164) for 30 minutes. Mouse IgG and IgM-coupled beads were incubated in assay buffer for 30 minutes. After incubation, 96-well-plate was placed on the magnetic ring stand and incubated for 60 seconds for separation to occur. The supernatant was discarded, and wells were washed twice with 100 µl of the assay buffer. Mouse IgM coupled beads were incubated with Streptavidin-R-Phycoerythrin Conjugate (SAPE) at 1.5 equivalent concentrations of biotinylated goat anti-mouse IgM used in that particular well for 30 min. The 96-well-plate was placed on the magnetic ring stand and incubated for 60 s for capture of the magnetic particles to occur. The supernatant was discarded, and wells were washed twice with 100 µl of the assay buffer. Beads were solubilized in the assay buffer and analyzed using MAGPIX (Luminex).

The resulting bead sets had an equal amount of the same type of antigen. OVA, OVA-PEG_{10K}, and OVA-$POEGMA_{10K}$ bead sets had equal amounts of OVA, indicated by identical median fluorescence intensity (MFI) detected at varied mouse anti-OVA antibody concentrations **(Supplementary Fig. 32a)**. Similarly, exendin, exendin-PEG_{10K}, and exendin-$POEGMA_{10K}$ bead sets had equal amounts of exendin **(Supplementary Fig. 32b)**. Importantly, we confirmed that exendin-PEG_{10K}- and OVA-PEG_{10K}-conjugated bead sets had equal amounts of PEG **(Supplementary Fig. 32c)**. We also confirmed the conjugation of mouse IgG **(Supplementary Fig. 32d)** and mouse IgM **(Supplementary Fig. 32e)** on the positive control beads.

Optimization and validation of the LMI. The LMI was optimized in its background, specificity, sensitivity, precision, and linearity. The optimized assay was validated by performing a spike-and-recovery experiment.

Background. The Limit of Blank (LoB) was defined as median fluorescence intensity (MFI) of singleplex and multiplexed drug-coupled magnetic beads in assay buffer. Singlet LoB (SLoB) and multiplexed LoB (MLoB) were calculated by adding three standard deviations to the mean MFI in the assay buffer **(Supplementary Table 3)**. The highest SLoB was 42 MFI, roughly corresponding to 0.26% of MFI detected with anti-drug

antibodies, indicating that drug-coupled beads have a low fluorescence background. Importantly, SLoB and MLoB were not significantly different ($P>0.99$), indicating that multiplexing the beads does not affect their fluorescence background.

Specificity. We tested if the control antibodies (anti-exendin IgG, anti-OVA IgG, anti-PEG IgG, anti-mouse IgG, and anti-mouse IgM) showed any cross-reactivity to the drug-coupled beads by incubating singleplex and multiplexed beads with a single type or multiple types of antibodies. Cross-reactivity of a bead set to a control antibody was calculated as the percent MFI signal of a true positive bead set and was less than 1% for all drug-coupled beads at 1 μg ml^{-1} antibody concentration. This result indicated that the control reagents were of high specificity. Similarly, the assay buffer showed no cross-reactivity to anti-drug antibodies or drugs **(Supplementary Table 4)**.

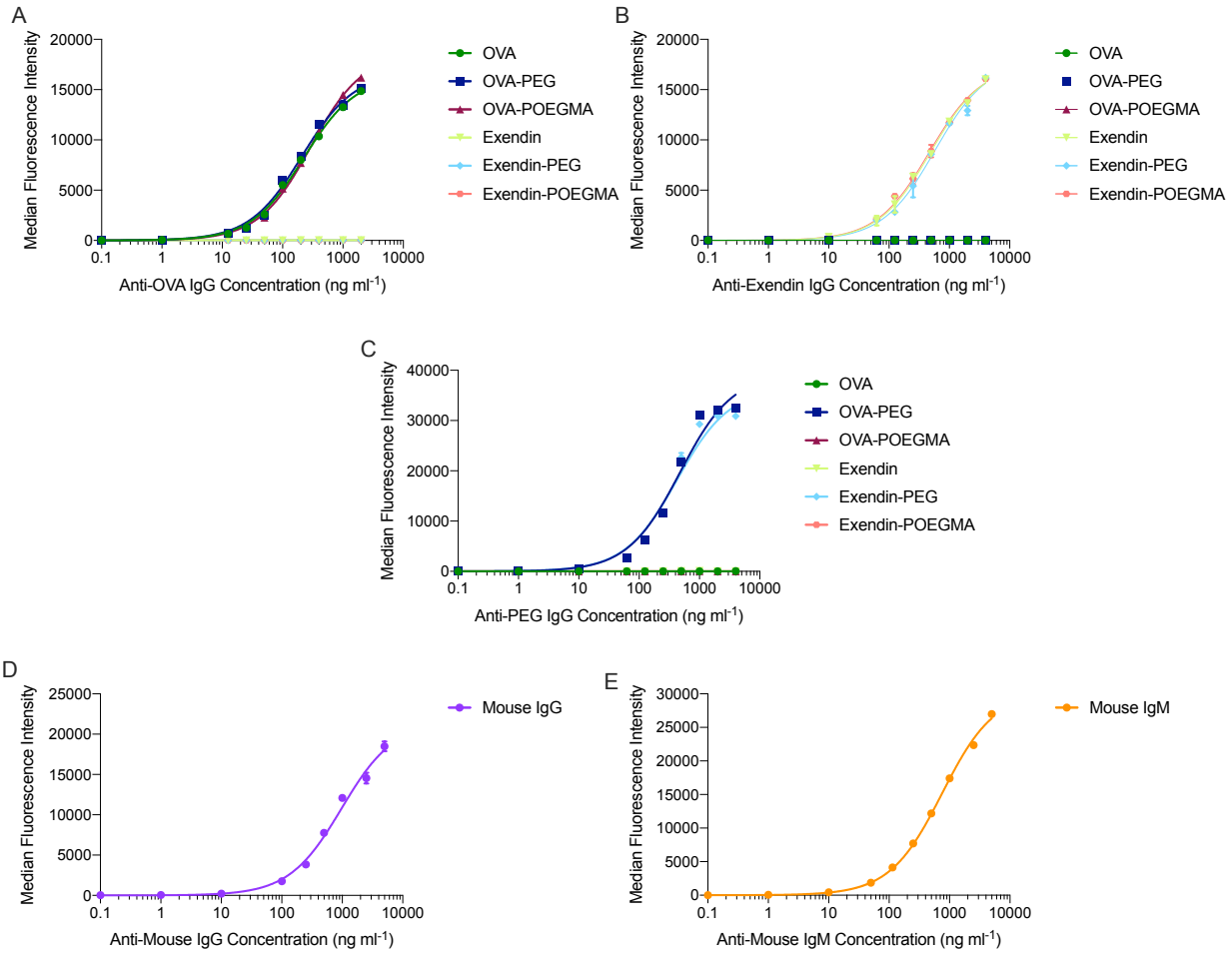

Supplementary Figure 32. Characterization of drug- and antibody-coupled beads used in Luminex multiplexed immunoassays. The amount of drug coupled was carefully titrated to ensure that the resulting bead sets had equal amounts of the same type of antigen, indicated by near-identical MFI detected at varied positive control antibody concentrations.

Supplementary Table 3. Background of the LMI. The Limit of Blank (LoB) was defined as MFI of singlet and multiplexed drug-coupled magnetic beads in assay buffer. SLoB and MLoB were calculated by adding three standard deviations to the mean MFI detected in the assay buffer. Data were analyzed using two-way repeated-measures ANOVA, followed by Tukey's multiple comparison test. $P<0.05$ was considered statistically significant. N/A (Not applicable).

Antigen/ Limit of Blank (LoB)	OVA	OVA-PEG$_{10K}$	OVA-POEGMA$_{10K}$	Exendin	Exendin-PEG$_{10K}$	Exendin-POEGMA$_{10K}$	Mouse IgG	Mouse IgM
Singleplex LoB	41.2	40.3	40.6	36.9	39.1	28.6	26.8	29.5
Multiplexed LoB	26.2	27.1	38.8	26.1	34.6	35.5	N/A	N/A

Supplementary Table 4. The specificity of the control antibodies used in the LMI. Cross-reactivity of a bead set to a control antibody was calculated as the percent MFI signal of a true positive bead set and assessed at 1 μg ml^{-1} control antibody concentration. Data represent the mean and SEM.

Singleplex Antigen Cross-Reactivity (%)								
Antigen/Anti-Drug Antibody	**OVA**	**OVA-PEG**	**OVA-POEGMA**	**Exendin**	**Exendin-PEG**	**Exendin-POEGMA**	**Mouse IgG**	**Mouse IgM**
Anti-OVA IgG	100±7.0	100±0.4	100±2.2	0.2±0.01	0.2±0.01	0.2±0.01	0.6±0.04	0.2±0.03
Anti-PEG IgG	0.5±0.1	234.5±0.5	0.6±0.1	0.2±0.01	280.4±4.2	0.6±0.06	0.5±0.04	0.2±0.02
Anti-Exendin IgG	0.2±0.02	0.3±0.1	0.2±0.04	100±1.4	100±2.25	100±5.47	0.5±0.02	0.2±0.06
Anti-Mouse IgG	0.2±0.01	0.2±0.02	0.1±0.01	0.2±0.02	0.2±0.02	0.2±0.01	100±6	0.2±0.02
Anti-Mouse IgM	0.2±0.01	0.2±0.02	0.2±0.02	0.2±0.02	0.2±0.02	0.1±0.02	0.7±0.07	100±9.3
Anti-OVA IgG + Anti-Exendin IgG	98.1±0.1	94.5±4.4	96.4±1.1	101.8±9.2	100.7±1	97.9±0.9	0.5±0.1	0.3±0.06
Anti-OVA IgG+ Anti-Exendin IgG + Anti-PEG IgG	98.4±6.1	314.3±7.7	96.0±9.4	102.2±2.5	377.2±0.3	103.5±4.1	0.6±0.07	0.2±0.2
Multiplexed Antigen Cross-Reactivity (%)								
Antigen/Anti-Drug Antibody	**OVA**	**OVA-PEG**	**OVA-POEGMA**	**Exendin**	**Exendin-PEG**	**Exendin-POEGMA**	**Mouse IgG**	**Mouse IgM**
Anti-OVA IgG	100±3	100±4.6	100±1.4	0.2±0.02	0.2±0.05	0.2±0.03	0.5±0.1	0.1±0.01
Anti-PEG IgG	0.2±0.03	231±2.8	0.24±0.1	0.65±0.02	233.8±2.7	0.35±0.03	0.5±0.02	0.1±0.02
Anti-Exendin IgG	0.2±0.03	0.2±0.01	0.2±0.05	100±1.2	100±1.2	100±2.4	0.5±0.01	0.2±0.01
Anti-Mouse IgG	0.1±0.1	0.07±0.08	0.2±0.01	0.1±0.07	0.2±0.01	0.1±0.09	100±2.2	0.9±0.05
Anti-Mouse IgM	0.1±0.04	0.2±0.01	0.2±0.02	0.2±0.1	0.2±0.01	0.2±0.03	0.5±0.03	100±0.7
Anti-OVA IgG + Anti-Exendin IgG	96.3±2	241±1.6	97.3±3.2	93.8±2.6	239±4.3	94.5±4.2	0.2±0.01	0.1±0.1
Anti-OVA IgG+ Anti-Exendin IgG + Anti-PEG IgG	94.3±1.9	327.3±7.2	100.8±1.9	100.9±0.6	346.3±4.6	97.9±4.8	0.6±0.3	0.2±0.08

Sensitivity. The sensitivity of the immunoassay was assessed at varying concentrations of the control antibodies. The Limit of Detection (LoD) was defined as the minimum detectable control antibody dose for a particular drug-coupled bead and calculated for each bead set as mean antibody concentration plus three standard deviations. LoD was below 1.5 ng ml^{-1} for all antigens (**Supplementary Table 5**), indicating that the assay has high sensitivity. The lower limit of quantification (LLoQ) and upper limit of quantification (ULoQ) were defined *as the* as the minimum and maximum antibody concentration detected in the assay's

linear working range plus three standard deviations*, respectively, and* demarcate the lower and upper boundaries of the assay for each bead set.

Supplementary Table 5. The sensitivity of the LMI. The LoD was defined as the minimum detectable control antibody dose for a particular drug-coupled bead and calculated for each bead set as mean antibody concentration plus three standard deviations. The LLoQ and ULoQ defined the lower and upper boundaries of the assay's linear working range for each bead set. N/A (Not applicable).

Antigen/ Sensitivity (ng ml^{-1})	OVA	OVA-PEG$_{10K}$	OVA-POEGMA$_{10K}$	Exendin	Exendin-PEG$_{10K}$	Exendin-POEGMA$_{10K}$	Mouse IgG	Mouse IgM
Anti-OVA LoD	0.315	0.289	0.426	N/A	N/A	N/A	N/A	N/A
Anti-OVA LLoQ	0.999	1.063	0.935	N/A	N/A	N/A	N/A	N/A
Anti-OVA ULoQ	119.8	123.1	115.0	N/A	N/A	N/A	N/A	N/A
Anti-PEG LoD	N/A	0.514	N/A	N/A	0.450	N/A	N/A	N/A
Anti-PEG LLoQ	N/A	1.001	N/A	N/A	1.002	N/A	N/A	N/A
Anti-PEG ULoQ	N/A	568.3	N/A	N/A	507.5	N/A	N/A	N/A
Anti-Exendin LoD	N/A	N/A	N/A	1.248	1.452	1.397	N/A	N/A
Anti-Exendin LLoQ	N/A	N/A	N/A	5.276	5.185	5.191	N/A	N/A
Anti-Exendin ULoQ	N/A	N/A	N/A	103.3	124.4	129.4	N/A	N/A
Anti-mouse IgG LoD	N/A	N/A	N/A	N/A	N/A	N/A	0.126	N/A
Anti-mouse IgG LLoQ	N/A	N/A	N/A	N/A	N/A	N/A	1.171	N/A
Anti-mouse IgG ULoQ	N/A	N/A	N/A	N/A	N/A	N/A	500.1	N/A
Anti-mouse IgM LoD	N/A	N/A	N/A	N/A	N/A	N/A	N/A	0.326
Anti-mouse IgM LLoQ	N/A	N/A	N/A	N/A	N/A	N/A	N/A	0.997
Anti-mouse IgM ULoQ	N/A	N/A	N/A	N/A	N/A	N/A	N/A	169.6

Linearity. The assay's linearity was determined by assessing whether assay values were proportional to the analyte concentration. It was defined as the goodness of fit (R^2) of at least four dilutions of plasma or control antibodies in the assay buffer. R^2 values were greater than 0.98 for all bead sets, indicating that working conditions remained in the assay's dynamic range (**Supplementary Table 6**).

Supplementary **Table 6. The linearity of the LMI.** Linearity was defined as the R^2 of at least four dilutions of plasma or control antibodies in the assay buffer. Not applicable (N/A).

Linearity Correlation Coefficient in Assay Buffer								
Antigen/Anti-Drug Antibody	**OVA**	**OVA-PEG$_{10K}$**	**OVA-POEGMA$_{10K}$**	**Exendin**	**Exendin-PEG$_{10K}$**	**Exendin-POEGMA$_{10K}$**	**Mouse IgG**	**Mouse IgM**
Anti-OVA IgG	0.999	0.999	0.993	N/A	N/A	N/A	N/A	N/A
Anti-PEG IgG	N/A	0.999	N/A	N/A	0.985	N/A	N/A	N/A
Anti-Exendin IgG	N/A	N/A	N/A	0.999	0.998	0.999	N/A	N/A
Anti-Mouse IgG	N/A	N/A	N/A	N/A	N/A	N/A	0.999	N/A
Anti-Mouse IgM	N/A	N/A	N/A	N/A	N/A	N/A	N/A	0.984
Linearity Correlation Coefficient in Immunized Mice Plasma								
Antigen/ Plasma	**OVA**	**OVA-PEG$_{10K}$**	**OVA-POEGMA$_{10K}$**	**Exendin**	**Exendin-PEG$_{10K}$**	**Exendin-POEGMA$_{10K}$**	**Mouse IgG**	**Mouse IgM**
Anti-OVA	0.994	0.987	0.993	N/A	N/A	N/A	N/A	N/A
Anti-OVA-PEG	0.990	0.976	0.995	N/A	N/A	N/A	N/A	N/A
Anti-OVA-POEGMA	0.993	0.985	0.994	N/A	N/A	N/A	N/A	N/A
Anti-Exendin	N/A	N/A	N/A	N/S	NS	N/S	N/A	N/A
Anti-Exendin-PEG	N/A	N/A	N/A	N/S	0.990	N/S	N/A	N/A
Anti-Exendin-POEGMA	N/A	N/A	N/A	N/S	N/S	N/S	N/A	N/A

Precision. Precision was determined by assessing the repeatability and the reproducibility of the assay and is defined as the intra-assay and inter-assay variability. Intra-assay variability (%CV) was calculated by dividing the standard deviation of anti-drug IgG concentration measured using drug-coupled beads (*n*=9) on the same plate by its mean. Inter-assay variability (%CV) was calculated by dividing the standard deviation of anti-drug IgG concentration measured using drug-coupled beads on three different plates (*n*=3) by its mean. Intra-assay and inter-assay variabilities were 6.57% and 9.57% for all antigens, indicating that the assay had high precision (**Supplementary Table 7**).

Supplementary Table 7. The precision of the LMI. Precision was determined by assessing the repeatability and the reproducibility of the assay and defined as intra-assay and inter-assay variability.

Spiked Control Reagent	Intra-Assay Variability (%CV)	Inter-Assay Variability (%CV)
Anti-OVA IgG + Anti-Exendin IgG + Anti-PEG IgG	<6.57	<9.57

Validation. The optimized multiplexed immunoassay was validated by performing a spike-and-recovery experiment. Briefly, PBS-treated mouse plasma was spiked with 25 ng ml^{-1} of exendin, OVA, and PEG antibodies the percent drug recovered from the assay at varying dilutions was calculated. The % recovery

was 105.4 ± 9.6 in the assay buffer and 102 ± 7.7 in the plasma, validating the assay performance (**Supplementary Table 8**).

Supplementary Table 8. *The* validation of the optimized LMI. The optimized multiplexed immunoassay was validated by performing a spike-and-recovery experiment. Data represent the mean and standard deviation.

Spiked Control Reagent	Recovery in Diluent (%)	Recovery in Plasma (%)
Anti-OVA IgG + Anti-Exendin IgG + Anti-PEG IgG	105.4±9.6	102±7.7

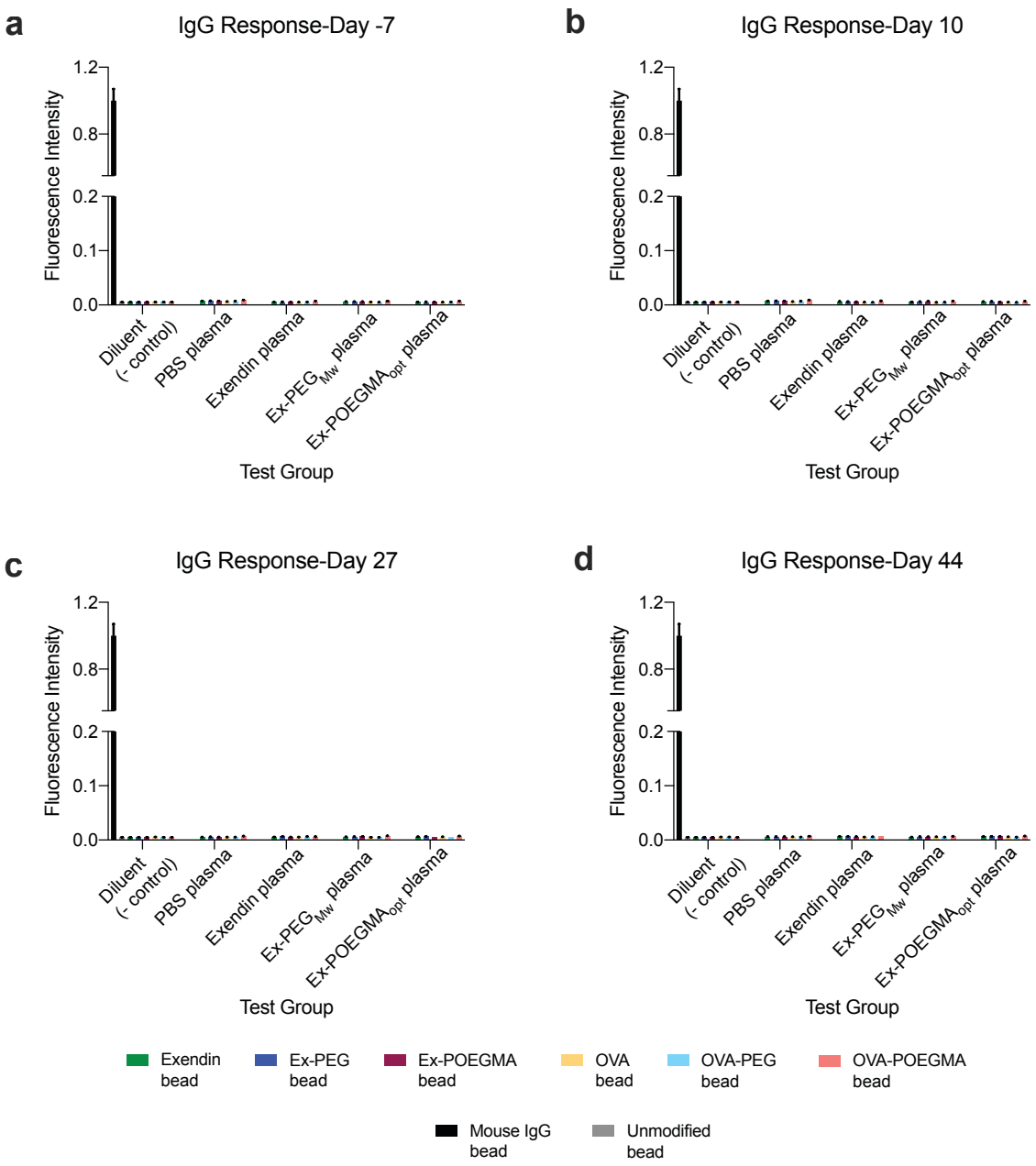

401

402 **Supplementary Figure 33. Ex-POEGMA$_{opt}$ does not induce exendin- or POEGMA-specific IgGs.** IgG response on **(A)** Day -7, **(B)**
403 Day 10, **(C)** Day 27, and **(D)** Day 44. Blood samples were collected from mice repeatedly treated with PBS, exendin, Ex-PEG$_{Mw}$,
404 and Ex-POEGMA$_{opt}$. ADA response was analyzed using a LMI. Ex-PEG- and Ex-POEGMA-coupled beads were used to determine
405 ADAs induced towards the entire conjugate (*i.e.,* anti-exendin and anti-polymer (PEG or POEGMA)). OVA-PEG- and OVA-POEGMA-
406 coupled beads were used to determine ADAs induced towards PEG or POEGMA, respectively. The OVA-coupled bead was used
407 as a negative control for cross-reactivity towards OVA. Data represent the mean ADA response induced in each mouse and the

SEM. Data were analyzed by two-way repeated-measures ANOVA, followed by *post-hoc* Tukey's multiple comparison test. Data were considered statistically significant when $p<0.05$.

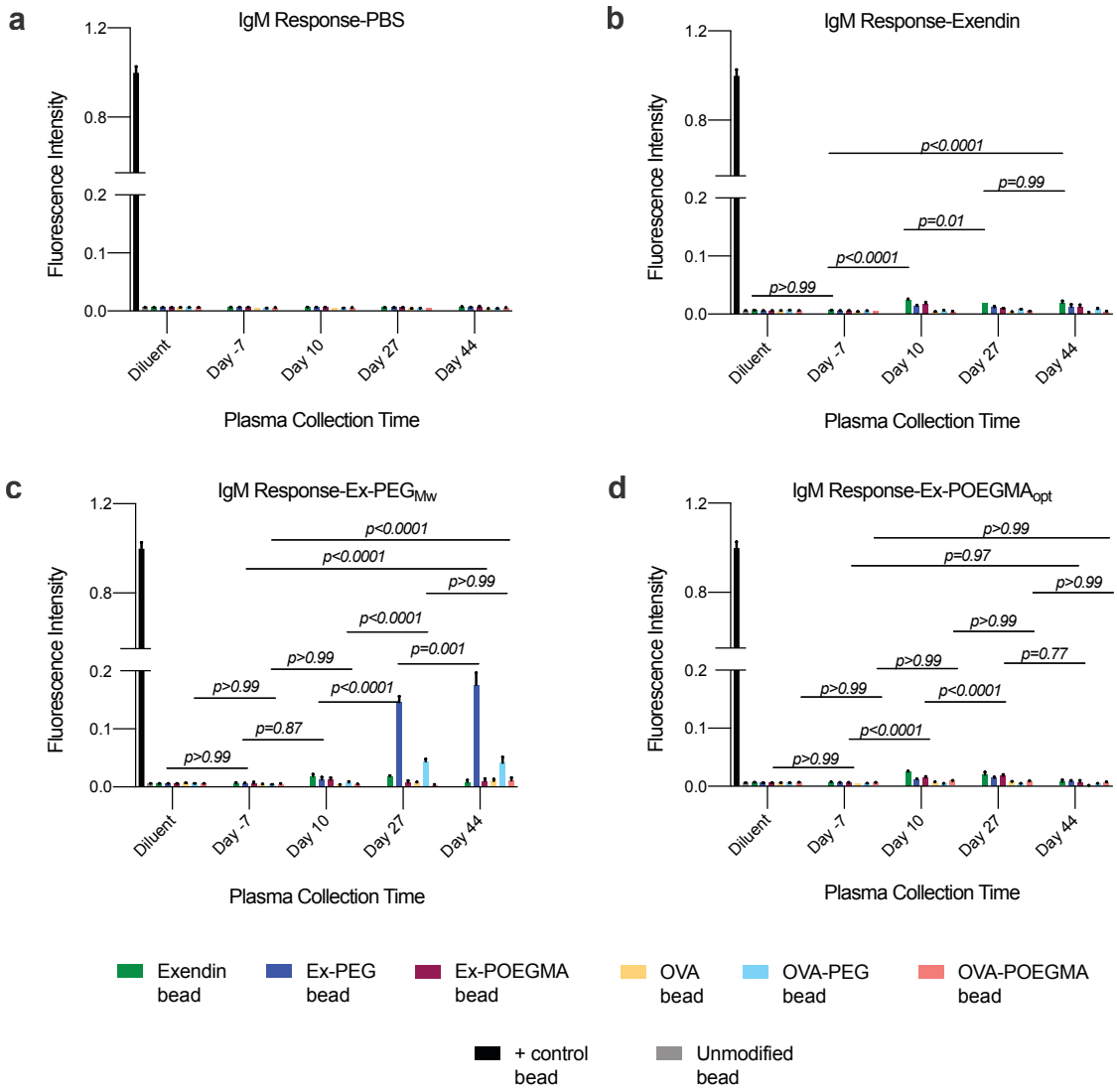

Supplementary Figure 34. Development of IgM responses towards exendin variants over time. IgM response towards **(A)** PBS, **(B)** exendin, **(C)** Ex-PEG$_{Mw}$, and **(D)** Ex-POEGMA$_{opt.}$ Blood samples were collected from mice repeatedly treated with PBS, exendin, Ex-PEG$_{Mw}$, and Ex-POEGMA$_{opt}$. ADA response analyzed using a LMI. Ex-PEG- and Ex-POEGMA-coupled beads were used to determine ADAs induced towards the entire conjugate (*i.e.,* anti-exendin and anti-polymer (PEG or POEGMA)). OVA-PEG- and OVA-POEGMA-coupled beads were used to determine ADAs induced towards PEG or POEGMA, respectively. The OVA-coupled bead was used as a negative control for cross-reactivity towards OVA. Different panels represent mice immunized with the various materials, while the different colored bars are what was applied in the multiplex assay. Data represent the mean ADA response

induced in each mouse and the SEM. Data were analyzed by two-way repeated-measures ANOVA, followed by *post-hoc* Tukey's multiple comparison test. Data were considered statistically significant when $p<0.05$.

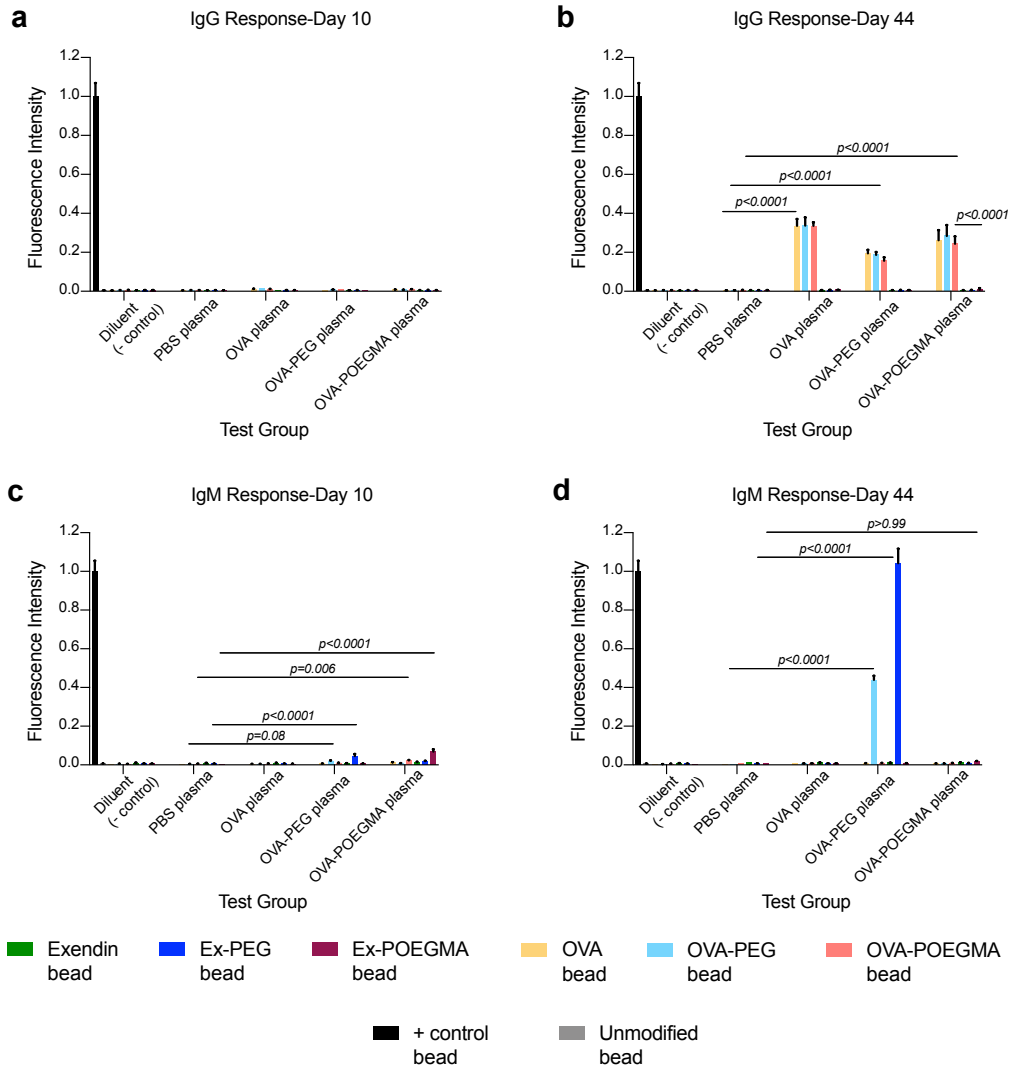

Supplementary Figure 35. OVA-POEGMA does not induce anti-POEGMA antibodies except a mild and transient IgM response. IgM response on **(A)** Day 10, **(B)** Day 27, and **(C)** Day 44. IgG response on **(D)** Day 10, **(E)** Day 27, and **(F)** Day 44. Blood samples were collected from C57BL/6J mice treated with OVA, OVA-PEG, and OVA-POEGMA (2.34 μM) at an equivalent dose of 9.6 nmol kg^{-1} bodyweight using an equivalent volume of PBS as a negative control. Blood collection and drug injection followed the timeline given in Figure 6a. ADA response analyzed using a LMI. OVA-PEG- and OVA-POEGMA-coupled beads were used to determine ADAs induced towards the entire conjugate (*i.e.,* anti-OVA and anti-polymer (PEG or POEGMA)). Ex-PEG- and Ex-POEGMA-coupled

beads were used to determine ADAs induced towards PEG or POEGMA, respectively. The exendin-coupled bead was used as a negative control for cross-reactivity towards OVA. Data represent the mean ADA response induced in each mouse and the SEM. Data were analyzed by two-way repeated-measures ANOVA, followed by *post-hoc* Tukey's multiple comparison test. Data were considered statistically significant when $p<0.05$.

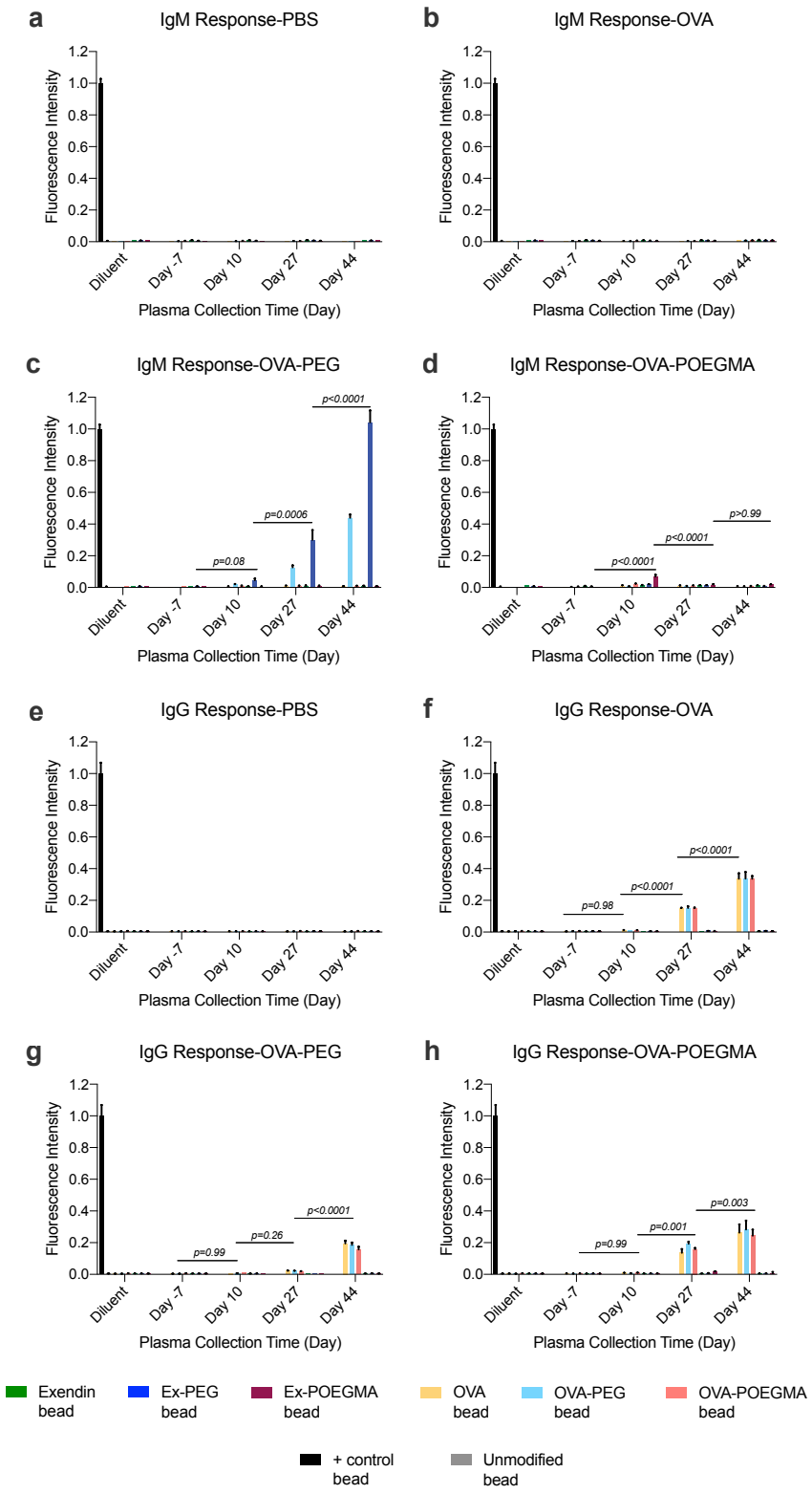

Supplementary Figure 36. Development of immune response towards OVA-based treatments over time. IgM response towards **(A)** PBS, **(B)** OVA, **(C)** OVA-PEG, and **(D)** OVA-POEGMA. IgG response towards **(E)** PBS, **(F)** OVA, **(G)** OVA-PEG, and **(H)** OVA-

435 POEGMA. Blood samples were collected from C57BL/6J mice treated with OVA, OVA-PEG, and OVA-POEGMA at an equivalent
436 dose of 9.6 nmol kg^{-1} bodyweight using an equivalent volume of PBS as a negative control. Blood collection and drug injection
437 followed the timeline given in Figure 6a. ADA response analyzed using a LMI platform. OVA-PEG- and OVA-POEGMA-coupled
438 beads were used to determine ADAs induced towards the entire conjugate (*i.e.,* anti-OVA and anti-polymer (PEG or POEGMA)).
439 Ex-PEG- and Ex-POEGMA-coupled beads were used to determine ADAs induced towards PEG or POEGMA, respectively. The
440 exendin-coupled bead was used as a negative control for cross-reactivity towards OVA. Data represent the mean ADA response
441 induced in each mouse and the SEM. Data were analyzed by two-way repeated-measures ANOVA, followed by *post-hoc* Tukey's
442 multiple comparison test. Data were considered statistically significant when $p<0.05$.

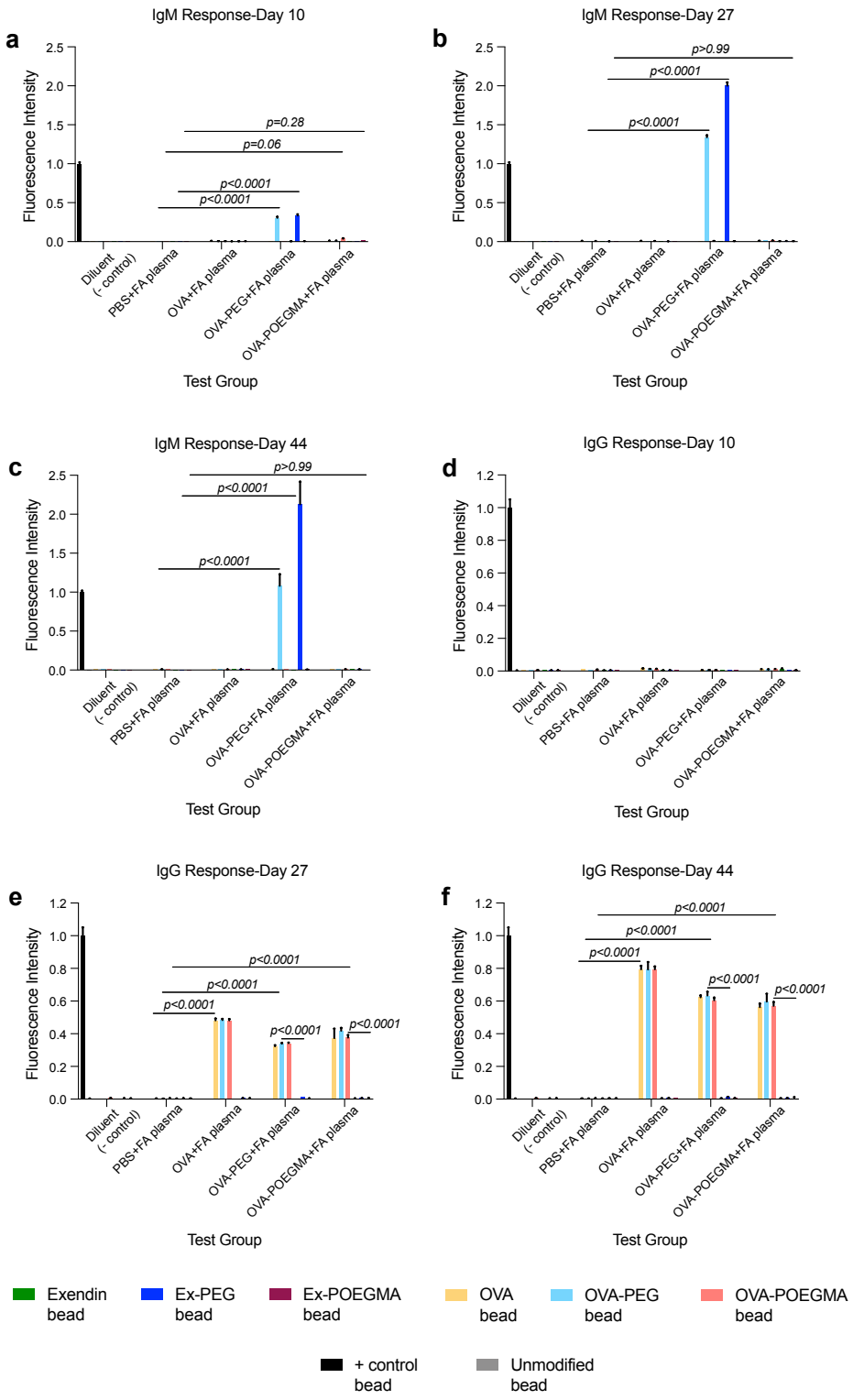

443

444 **Supplementary Figure 37. OVA-POEGMA administrated with FA does not induce anti-POEGMA antibodies except a mild and**

445 **transient IgM response**. IgM response on **(A)** Day 10, **(B)** Day 27, and **(C)** Day 44. IgG response on **(D)** Day 10, **(E)** Day 27, and **(F)**

Day 44. Blood samples were collected from C57BL/6J mice treated with equivalent doses of 1:1 (v/v) emulsions of OVA, OVA-PEG, and OVA-POEGMA in PBS and FA using an equivalent volume of PBS as a negative control. Blood collection and drug injection followed the timeline given in Figure 6a. ADA response analyzed using a Luminex multiplexed immunoassay platform. OVA-PEG- and OVA-POEGMA-coupled beads were used to determine ADAs induced towards the entire conjugate (*i.e.,* anti-OVA and anti-polymer (PEG or POEGMA)). Ex-PEG- and Ex-POEGMA-coupled beads were used to determine ADAs induced towards PEG or POEGMA, respectively. The exendin-coupled bead was used as a negative control for cross-reactivity towards OVA. Data represent the mean ADA response induced in each mouse and the SEM. Data were analyzed by two-way repeated-measures ANOVA, followed by *post-hoc* Tukey's multiple comparison test. Data were considered statistically significant when $p<0.05$.

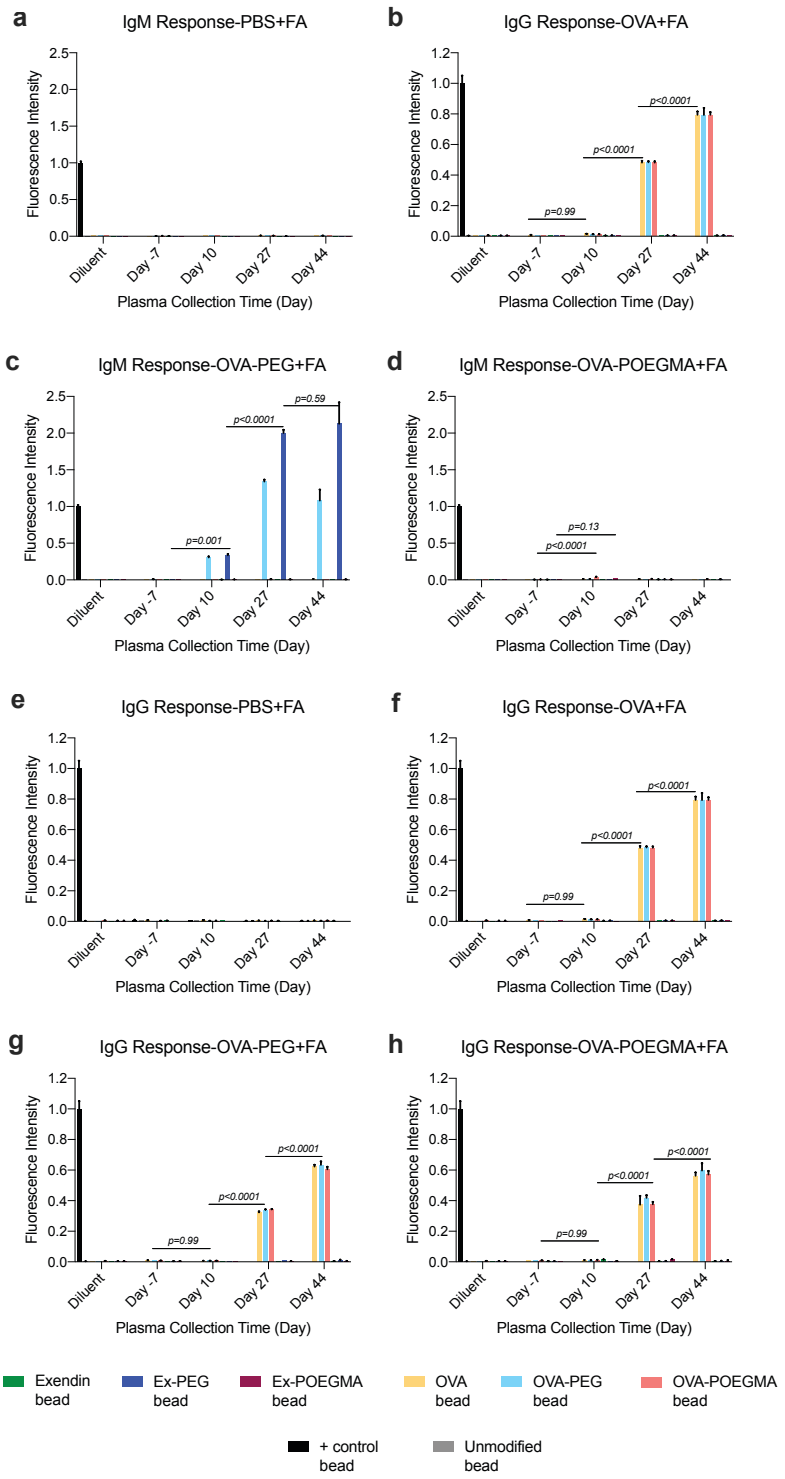

Supplementary Figure 38. Development of immune response towards OVA variants administered as FA emulsions over time. IgM response towards **(A)** PBS, **(B)** OVA, **(C)** OVA-PEG, and **(D)** OVA-POEGMA. IgG response towards **(E)** PBS, **(F)** OVA, **(G)** OVA-PEG, and **(H)** OVA-POEGMA. Blood samples were collected from C57BL/6J mice treated with equivalent doses of 1:1 (v/v)

458 emulsions of OVA, OVA-PEG, and OVA-POEGMA in PBS and FA using an equivalent volume of PBS as a negative control. Blood
459 collection and drug injection followed the timeline given in Figure 6a. ADA response analyzed using a LMI. OVA-PEG- and OVA-
460 POEGMA-coupled beads were used to determine ADAs induced towards the entire conjugate (*i.e.,* anti-OVA and anti-polymer
461 (PEG or POEGMA)). Ex-PEG- and Ex-POEGMA-coupled beads were used to determine ADAs induced towards PEG or POEGMA,
462 respectively. The exendin-coupled bead was used as a negative control for cross-reactivity towards OVA. Data represent the mean
463 ADA response induced in each mouse and the SEM. Data were analyzed by two-way repeated-measures ANOVA, followed by
464 *post-hoc* Tukey's multiple comparison test. Data were considered statistically significant when $p<0.05$.

Section 6. Effect of ADAs on the long-term efficacy

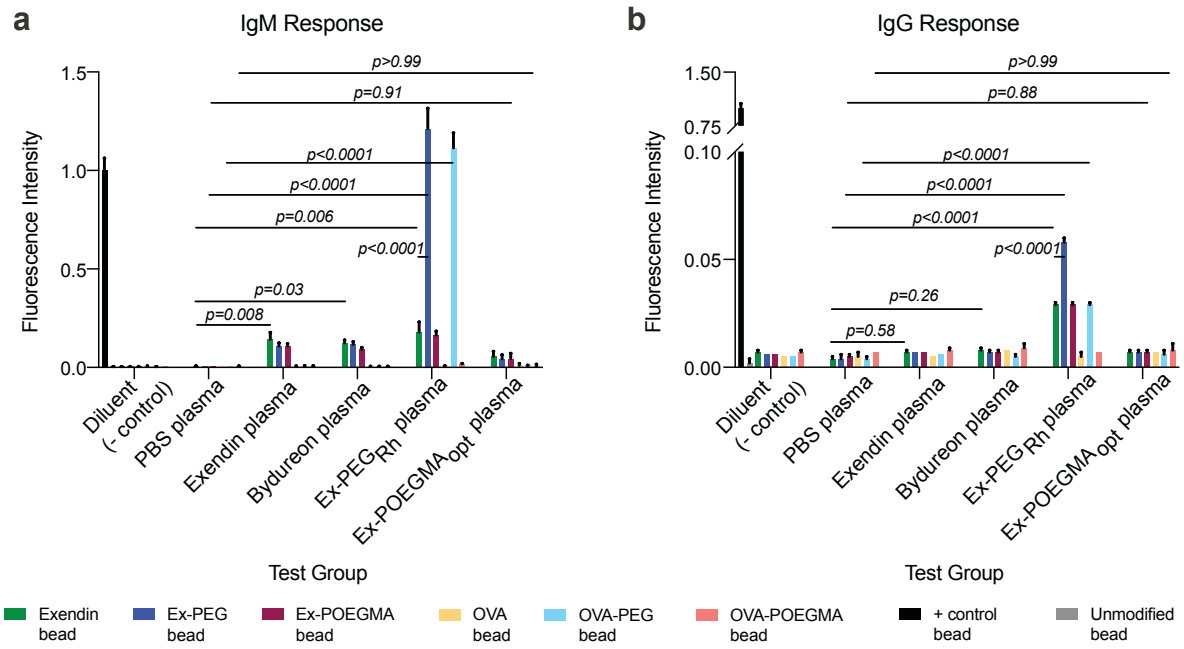

Supplementary Figure 39. Ex-POEGMA$_{opt}$ does not induce anti-POEGMA antibodies after long-term treatment. (A) IgM and **(B)** IgG response after weekly treatment of 6-week-old *db/db* mice (*n*=5) for eight weeks with equivalent drug dose of exendin, Bydureon, Ex-PEG$_{Rh}$, and Ex-POEGMA$_{opt,}$ and an equivalent volume of PBS as a negative control. Blood samples were collected ten days after the last drug injection. ADA response was measured by a LMI. Ex-PEG- and Ex-POEGMA-coupled beads were used to determine ADAs induced towards the entire conjugate (*i.e.,* anti-exendin and anti-polymer (PEG or POEGMA)). OVA-PEG- and OVA-POEGMA-coupled beads were used to determine ADAs induced towards PEG or POEGMA, respectively. The OVA-coupled bead was used as a negative control for cross-reactivity towards OVA. Data represent the mean of the ADA response induced in each mouse and the error bars are the SEM. Data were analyzed by two-way repeated-measures ANOVA, followed by *post-hoc* Tukey's multiple comparison test. Data were considered statistically significant when p<0.05.

Design, optimization, and validation of a cell-based neutralizing antibody assay.

Assay Design. The presence of neutralizing antibodies (NAb) was tested in long-term treated mice sera. Nabs were analyzed using the in vitro cell-based assay described in Methods with minor modifications.[2] Briefly, the mice serum samples were incubated with exendin, Ex-PEG_{Mw}, or Ex-$POEGMA_{opt}$ for 2 h at room temperature. HEK293/CRE-Luc/GLP1R cells were then treated with the serum: drug mixtures (10% v/v) for 5 h at a final concentration of the drugs' respective half-maximal effective concentration (EC_{50}), followed by measurement of luminescence from the cells. This assay allowed us to determine the binding antibodies' neutralizing ability, such that if there were NAbs present, they interacted with the drugs and blocked their binding to GLP1R, preventing cAMP induction and leading to a decrease in luminescence.

Assay optimization. The NAb assay was optimized in terms of matrix interference and sensitivity.

Matrix interference. The matrix interference was tested in terms of HEK293/CRE-Luc/GLP1R cells' ability to respond to a fixed concentration of exendin at varying dilutions of PBS-treated C57BL/6J mice sera. We found that mice sera $\leq$ 5% (volume) did not significantly affect cell behavior (data not shown). Therefore, the final serum volume was kept constant at 5% across all assays.

Sensitivity. The sensitivity of the cell-based neutralizing antibody assay was tested using anti-exendin (NBP1-05179H; Novus Biologicals) and anti-PEG (ab195350; Abcam) antibodies as positive controls and anti-OVA antibody (ab17293; Abcam) as a negative control. Briefly, exendin, Ex-PEG_{Mw}, or Ex-$POEGMA_{opt}$ were preincubated with varied concentrations of anti-exendin, anti-PEG, and anti-OVA antibodies, which were diluted in 5% PBS-treated C57BL/6J mice sera, followed by treating HEK293/CRE-Luc/GLP1R cells and measuring luminescence. The luminescence signal measured from cells in each treatment group was represented as the percentage of the mean signal of cells treated without antibodies **(Supplementary Fig. 40)**. Anti-exendin antibodies inhibited exendin **(Supplementary Fig. 40a)**, Ex-PEG_{Mw} **(Supplementary Fig. 40b)**, or Ex-$POEGMA_{opt}$ **(Supplementary Fig. 40c)**, while anti-OVA antibodies did not have any effect on the

drugs' activity. Anti-PEG antibodies only inhibited Ex-PEG_{Mw} **(Supplementary Fig. 40b)** and did not affect the activity of exendin **(Supplementary Fig. 40a)** and Ex-$POEGMA_{opt}$ **(Supplementary Fig. 40c)**. The assay sensitivity was defined as the half-maximal inhibitory concentration (IC_{50}) of the antibodies and was summarized in **Supplementary Table 9**. The assay was more sensitive for exendin (7.2 $\pm$ 1.1 nM) than Ex-PEG_{Mw}(26.9 $\pm$ 5.3 nM) and Ex-$POEGMA_{opt}$ (23.5 $\pm$ 3.1 nM) due to the lower concentration of exendin (0.15 nM) used in the assay than Ex-PEG_{Mw} (2.7 nM) and Ex-$POEGMA_{opt}$ (2.8 nM). The molar equivalent of anti-exendin antibody needed to inhibit Ex-PEG_{Mw} (10.0 $\pm$ 2.0) and Ex-$POEGMA_{opt}$ (8.4 $\pm$ 1.1) half-maximally was higher than exendin (48 $\pm$ 7.3) due to the steric hindrance imparted on exendin by conjugated PEG and POEGMA. The assay sensitivity for anti-PEG antibodies was 28.3 $\pm$ 3.5 nM, which corresponded to the 10.5 $\pm$ 1.3 molar equivalent of Ex-PEG_{Mw}.

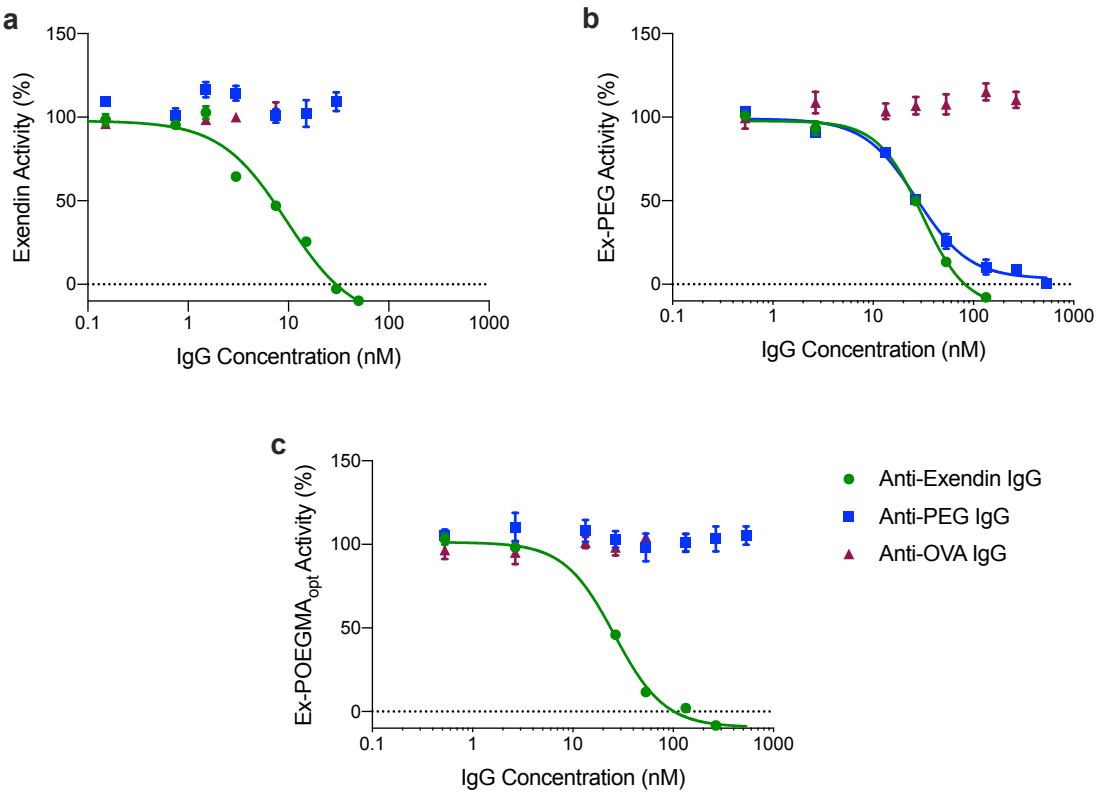

509

510 **Supplementary Figure 40. The sensitivity of a NAb assay.** Exendin, Ex-PEG$_{Mw}$, and Ex-POEGMA$_{opt}$ were preincubated with varied
511 concentrations of anti-exendin, anti-PEG, and anti-OVA antibodies in PBS-treated C57BL/6J mice sera, followed by treating
512 HEK293/CRE-Luc/GLP1R cells with the serum: drug mixtures (10% v/v) for 5 hours at a final concentration of the drugs' respective
513 EC$_{50}$s and measuring luminescence. The luminescence signal derived from each treatment group was represented as the
514 percentage of the mean signal of cells treated without antibodies. Data were fitted to a non-linear curve fit using GraphPad Prism
515 8 software.

516 **Supplementary Table 9. Summary of results of a cell-based neutralizing antibody assay.** Assay sensitivity was calculated from
517 the data shown in Supplementary Figure 41. Data represent the mean and the SEM. Data were fitted to a non-linear curve fit to
518 calculate the half-maximal inhibitory concentration (IC$_{50}$) of the antibodies using GraphPad Prism 8 software. Not applicable (n/a).

Treatment	Anti-Exendin IgG IC$_{50}$ (nM)	Fold Anti-Exendin IgG for IC$_{50}$	Anti-PEG IgG IC$_{50}$ (nM)	Fold Anti-PEG IgG for IC$_{50}$
Exendin	7.2 ± 1.1	48 ± 7.3	n/a	n/a
Ex-PEG$_{Mw}$	26.9 ± 5.3	10.0 ± 2.0	28.3 ± 3.5	10.5 ± 1.3
Ex-POEGMA$_{opt}$	23.5 ± 3.1	8.4 ± 1.1	n/a	n/a

519

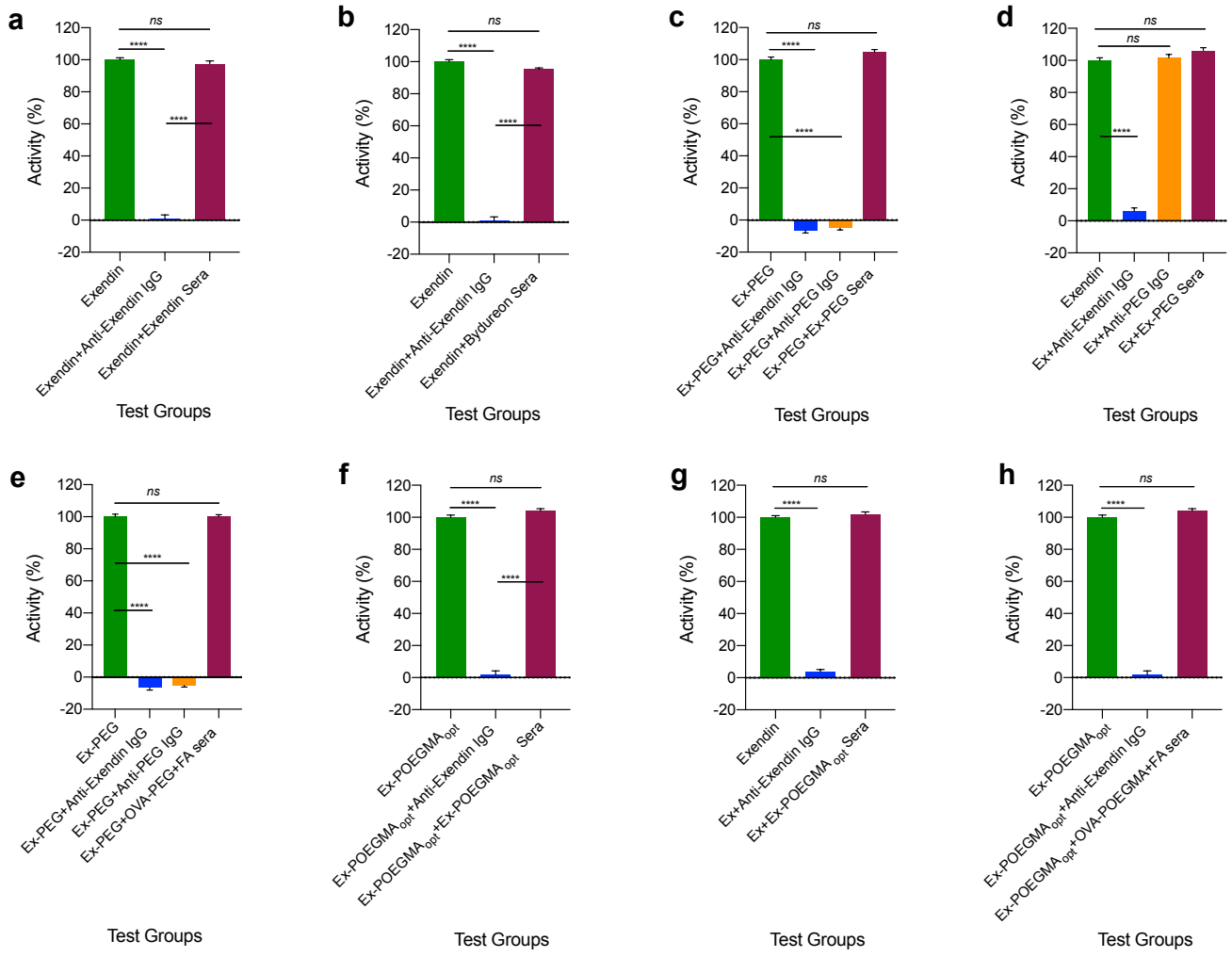

Supplementary Figure 41. Anti-exendin and anti-PEG antibodies are not neutralizing. *db/db* mice (*n*=5) long-term treated for with **(A)** exendin and **(B)** Bydureon did not elicit any neutralizing anti-exendin antibodies. *db/*db mice long-term treated with Ex-PEG$_{Rh}$ did not elicit neutralizing antibodies towards **(C)** Ex-PEG$_{Rh}$ or **(D)** exendin. **(E)** Anti-PEG antibody positive mice sera did not neutralize Ex-PEG$_{Rh}$ activity. Ex-POEGMA$_{opt}$-treated mice sera did not elicit any neutralizing antibodies reactive towards **(F)** Ex-POEGMA$_{opt}$ or **(G)** exendin. **(H)** Serum of C57BL/6J mice (*n*=10), which received repeated administrations of OVA-POEGMA: Freund's adjuvant, did not neutralize Ex-POEGMA$_{opt}$. The experiment was performed for each mouse serum separately (*n*=6 wells per mouse serum). Data represent the mean drug activity and the SEM. Data were analyzed by two-way ANOVA, followed by *post-hoc* Tukey's multiple comparison test. Data were considered statistically significant when $p<0.05$. Not significant (ns; $p>0.05$).

Section 7. Histopathological effects of treatments

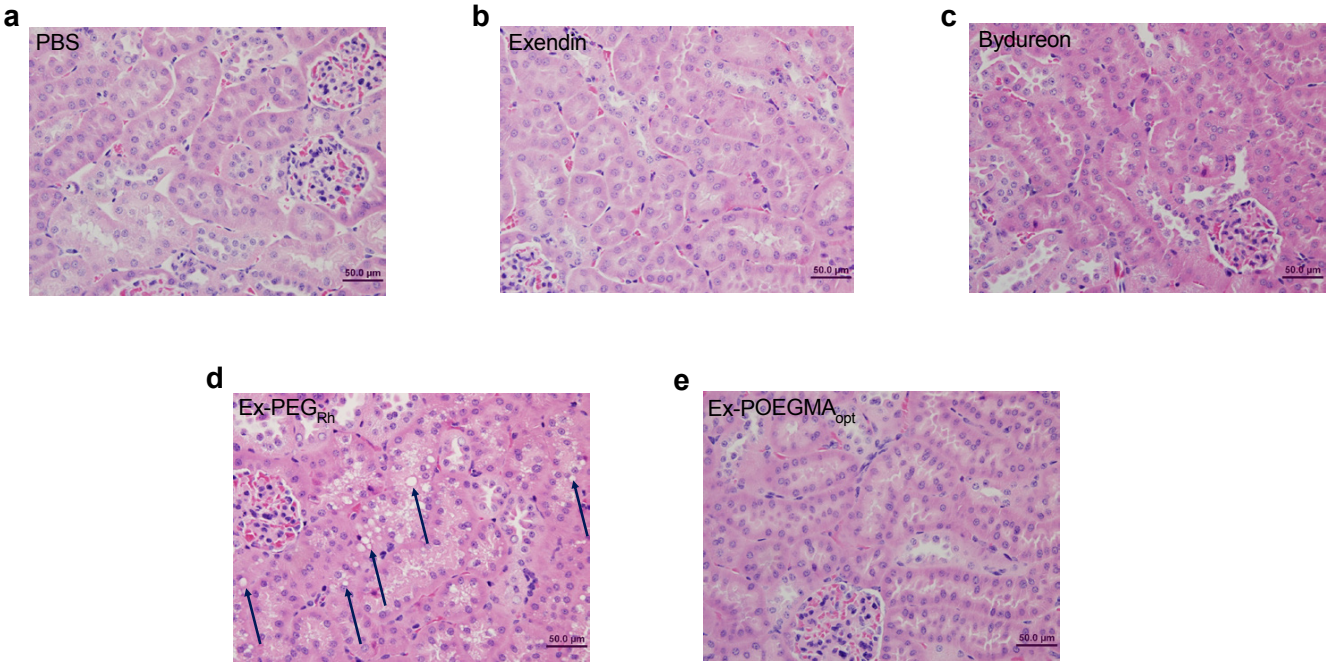

Supplementary Figure 42. Histopathological effects of treatments on the kidney. Representative histological slices of kidneys from long-term **(A)** PBS-, **(B)** exendin-, **(C)** Bydureon-, **(D)** Ex-PEG$_{Rh}$-, and **(E)** Ex-POEGMA$_{opt}$-treated *db/db* mice (*n*=3). The mice were treated weekly with *s.c.* injections of the treatments for eight weeks. At week 10, the mice were sacrificed, and organs were collected, followed by processing and staining with H&E. Compound induced renal changes were present in kidneys in each of the three Ex-PEG$_{Rh}$-treated mice. These vacuolar lesions, marked by arrows in (D) were prominent primarily within renal tubular epithelial cells of proximal tubules in the outer cortical region. No compound induced changes were noted in other treatments. Scale bar = 50µm.

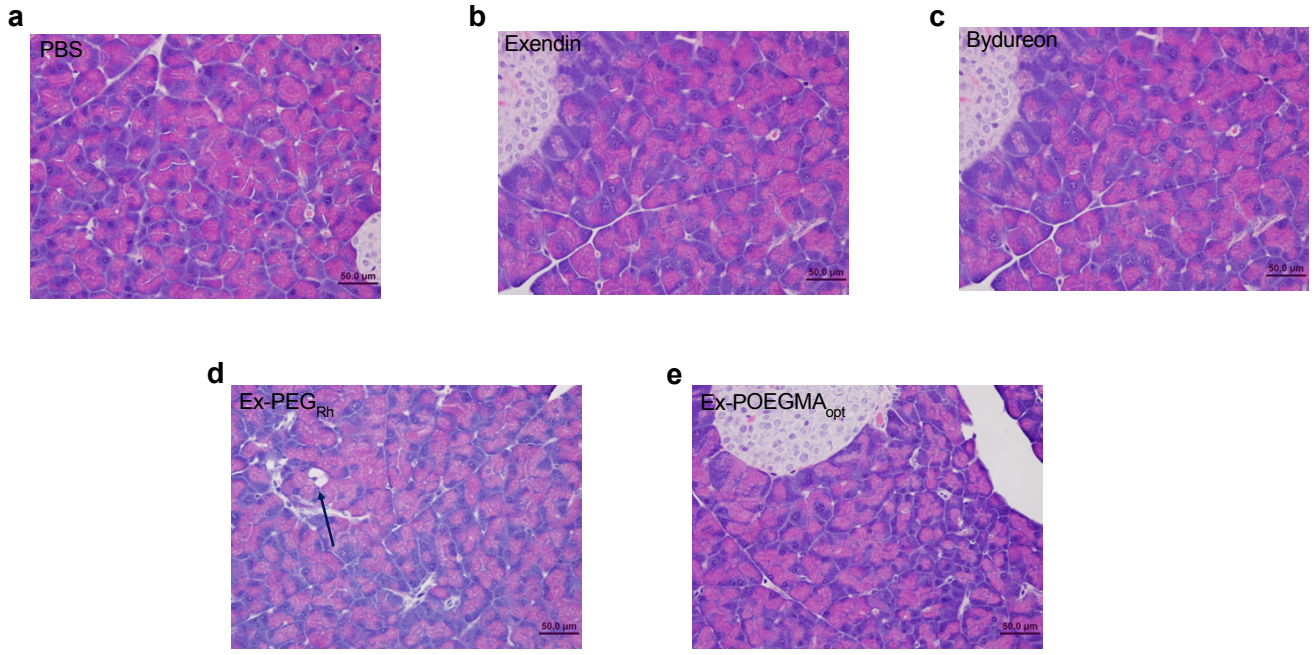

538

539 **Supplementary Figure 43. Histopathological effects of treatments on the pancreas.** Representative histological slices of
540 pancreas collected from long-term **(A)** PBS-, **(B)** exendin-, **(C)** Bydureon-, **(D)** Ex-PEG$_{Rh}$-, and **(E)** Ex-POEGMA$_{opt}$-treated *db/db* mice
541 (*n*=3). The mice were treated weekly with *s.c.* injections of the treatments for eight weeks. At week 10, the mice were sacrificed,
542 and organs were collected, followed by processing and H&E staining. Minimal compound induced vacuolar lesions, marked by
543 arrows in (D), were present in pancreases in each of the three Ex-PEG$_{Rh}$-treated mice. Scale bar = 50µm.

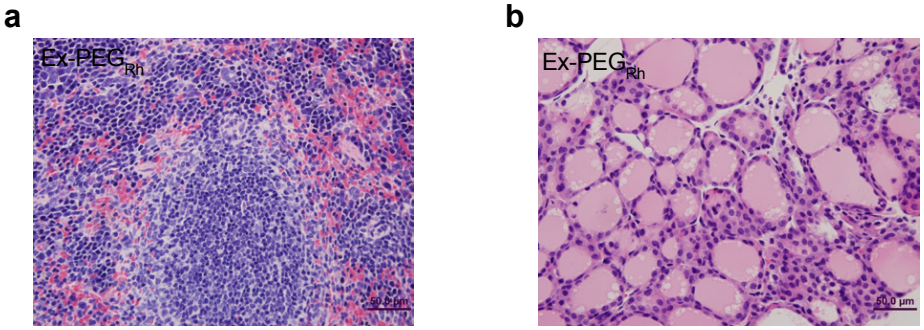

544

545 **Supplementary Figure 44. No Ex-PEG$_{Rh}$-induced histopathological alterations were identified in the (A) spleen and (B) thyroid**
546 **tissues.** Representative histological slices of pancreas collected from long-term Ex-PEG$_{Rh}$-treated *db/db* mice (*n*=3). The mice were
547 treated weekly with *s.c.* injections of the treatments for eight weeks. At week 10, the mice were sacrificed, and organs were
548 collected, followed by processing and H&E staining. Scale bar = 50µm.

References

1 Luminex. *xMAP CookBook*. 4th edn, (2018).

2 Buse, J. B. *et al.* Liraglutide Treatment Is Associated with a Low Frequency and Magnitude of Antibody Formation with No Apparent Impact on Glycemic Response or Increased Frequency of Adverse Events: Results from the Liraglutide Effect and Action in Diabetes (LEAD) Trials. *The Journal of Clinical Endocrinology & Metabolism* **96**, 1695-1702, doi:10.1210/jc.2010-2822 (2011).